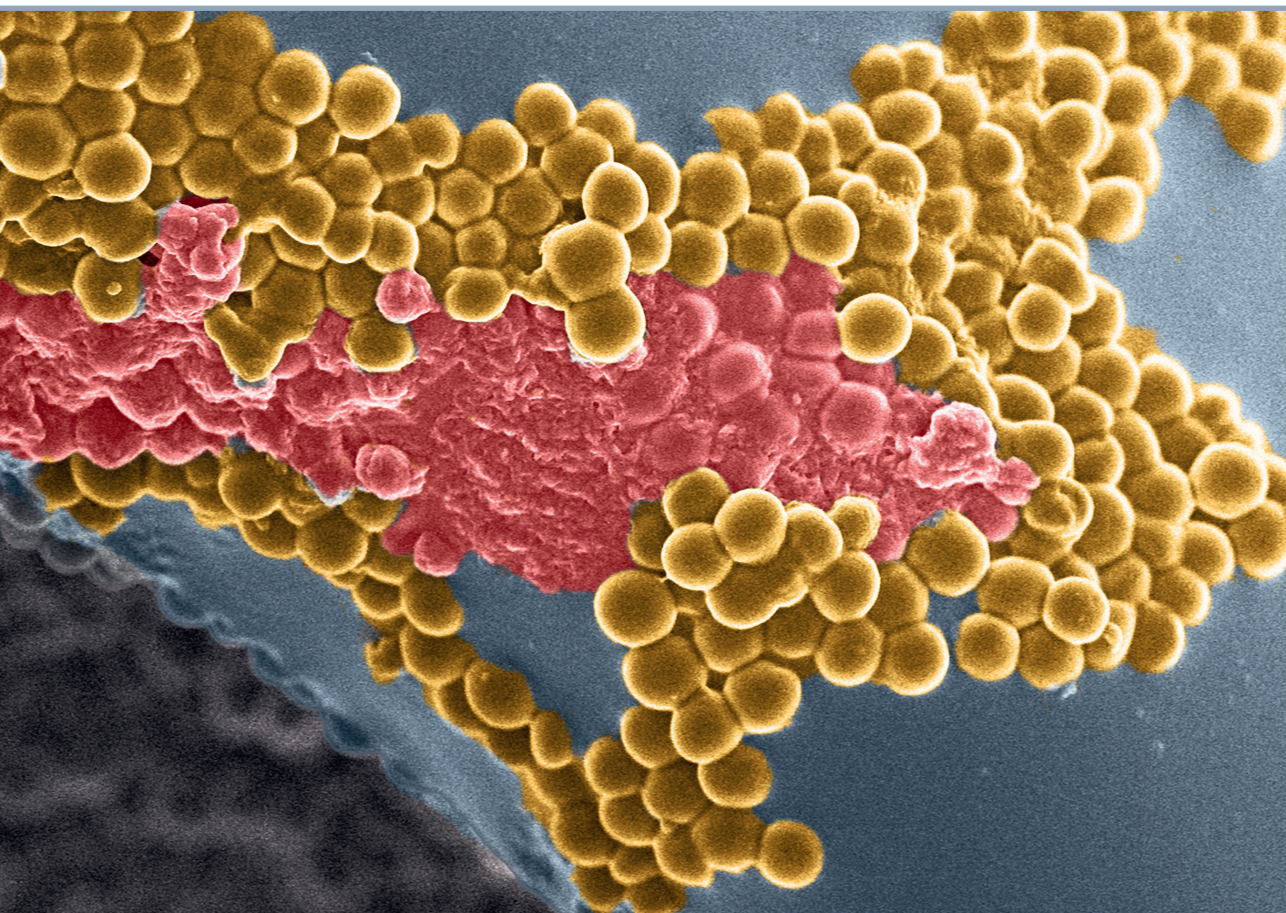


**Artemijs Ščeglovs**

**DEVELOPMENT OF INJECTABLE ANTIBACTERIAL  
HYDROGELS FOR TISSUE ENGINEERING**

Summary of the Doctoral Thesis



**RIGA TECHNICAL UNIVERSITY**

Faculty of Natural Sciences and Technology

Institute of Biomaterials and Bioengineering

**Artemijs Ščeglovs**

Doctoral Student of the Study Programme “Chemistry, Material Science and Engineering”

**DEVELOPMENT OF INJECTABLE  
ANTIBACTERIAL HYDROGELS FOR TISSUE  
ENGINEERING**

**Summary of the Doctoral Thesis**

Scientific supervisors

Professor Dr. sc. ing.

KRISTĪNE ŠALMA-ANCĀNE

Professor Dr. med.

JUTA KROIČA

RTU Press

Riga 2026

Ščeglovs, A. Development of Injectable Antibacterial Hydrogels for Tissue Engineering. Summary of the Doctoral Thesis. Riga: RTU Press, 2026. 45 p.

Published in accordance with the decision of the Promotion Council “P-02” of 13 October 2025, Minutes No. 04030-9.2/8.

The research conducted within the Doctoral Thesis has been supported by the Latvian Council of Science research project No. lzp-2020/1-0072 “Injectable Bioactive Biocomposites for Osteoporotic Bone Tissue Regeneration (inBioBone)” and European Union’s Horizon 2020 research and innovation programme under grant agreement No. 857287, Baltic Biomaterials Centre of Excellence (BBCE). The Doctoral Thesis has also been supported by the European Union’s Horizon 2020 research and innovation programme under grant agreement No. 952347 (RISEus2) and Ph.D. grant (C4835.Dok.1025) from the project No 5.2.1.1.i.0/2/24/I/CFLA/003 “Implementation of Consolidation and Management Changes at Riga Technical University, Liepaja University, Rezekne Academy of Technology, Latvian Maritime Academy and Liepaja Maritime College for the Progress towards Excellence in Higher Education, Science and Innovation” funded by the EU Recovery and Resilience Facility.



Cover picture by Dr. phys. Krišjānis Šmits.

<https://doi.org/10.7250/9789934372490>

ISBN 978-9934-37-249-0 (pdf)

## ACKNOWLEDGEMENTS

Heartfelt thanks to my family members and friends – I am so fortunate to have you, and I am proud of this! Thanks for your motivation, happiness, and love; for being an endless source of positive emotions; for giving me a way to step away from everything around me; and for always being there!

Thanks to my old band colleagues – Sofja, Karina, Eliza, Kristine A., Kristine I., Anda, Signe, Jana, Liga, Kristaps R., Agnese P., Lasma, Valentina, and Vita –, and colleagues from the new band – Anna R., Anastasia T., Ilijana, Theresa, Lauma, Jingzhi, Oznur, and Viktors – for your help, ideas, the off-work conversations, and jokes!

My immense gratitude to the people I worked and studied with for their invaluable input in the Doctoral Thesis – Jacek K. Wychowaniec, Claudia Siverino, Marco Chitto, Ingus Skadiņš, Inese Čakstiņa-Dzērve, Valdis Pirsko, Matteo D’Este, Fintan T. Moriarty, and Charlotte Edwards-Gayle!

Experienced scientists and my mentors – Prof. Jānis Ločs, Prof. Dagnija Loča, Assist. Prof. Arita Dubnika – and my supervisor – Prof. Juta Kroiča – Huge thanks to you for your advice, the time we spent together, and your wisdom in knowing when to praise and when to scold, when to help and when to step back and let me manage on my own.

From the bottom of my heart, I would like to express gratitude to my supervisor Prof. Kristīne Šalma-Ancāne for the work we have done together and experience we have gained, as well as for your ability to combine all of the above!

*“.....Where there is desire, there is gonna be a flame  
Where there is a flame, someone’s bound to get burned  
But just because it burns doesn’t mean you’re gonna die  
You’ve gotta get up and try, try, try.....”*

(Alecia Beth Moore, also known as Pink)/

# **DOCTORAL THESIS PROPOSED TO RIGA TECHNICAL UNIVERSITY FOR THE PROMOTION TO THE SCIENTIFIC DEGREE OF DOCTOR OF SCIENCE**

To be granted the scientific degree of Doctor of Science (Ph. D.), the present Doctoral Thesis has been submitted for defence at the open meeting of RTU Promotion Council on 20 February 2026 at 11:00, at the Faculty of Natural Sciences and Technology of Riga Technical University, 3 Paula Valdena Street, Room 272.

## **OFFICIAL REVIEWERS**

Tenured Professor Dr. sc. ing. Sergejs Gaidukovs  
Riga Technical University, Latvia

Vice-Dean of Sciences, Nephrologist, MD Ph. D. Karlis Racenis  
Riga Stradins University, Latvia

Ph. D. in Engineering Nihal Engin Vrana  
CEO at SPARTHA MEDICAL, France

## **DECLARATION OF ACADEMIC INTEGRITY**

I hereby declare that the Doctoral Thesis submitted for review to Riga Technical University for promotion to the scientific degree of Doctor of Science (Ph. D.) is my own. I confirm that this Doctoral Thesis has not been submitted to any other university for promotion to a scientific degree.

Artemijs Ščeglovs (signature)

Date: .....

The Doctoral Thesis has been elaborated as a collection of thematically related scientific publications completed by summaries in Latvian and English. The Doctoral Thesis unites four scientific publications. The scientific publications have been written in English, with a total volume of 174 pages, including supplementary data.

## ABSTRACT

Within the current Doctoral Thesis, synthesis and comprehensive characterisation of a novel hydrogel matrix of two chemically crosslinked, naturally derived biopolymers, antimicrobial polypeptide  $\epsilon$ -polylysine ( $\epsilon$ -PL) and biologically active hyaluronic acid (HA), have been performed. The main aim of the study is to develop non-antibiotic, inherently antibacterial hydrogel-based biomaterials for the repair and healing of infected tissue. The research has been carried out two main stages, involving the synthesis of covalently crosslinked  $\epsilon$ -PL/HA hydrogel matrix with further investigation of physicochemical properties such as molecular structure, morphology, gel fraction, swelling behaviour, as well as viscoelastic properties via rheological studies. Also, in the first stage, the effect of steam sterilisation on the physicochemical properties of the developed hydrogels has been investigated. Moreover, the *in vitro* antibacterial activity and cytotoxicity profile of the pure antimicrobial polypeptide  $\epsilon$ -PL and furtherly  $\epsilon$ -PL/HA hydrogels have been evaluated. Minimum inhibitory concentration (MIC), minimum bactericidal concentration (MBC) values and resistance development studies of pure  $\epsilon$ -PL, as well as antibacterial activity of the fabricated hydrogels have been evaluated in both fast-acting (at 24 h) and sustained (up to 168 h) timeframes against widely known Gram-negative and Gram-positive pathogenic bacterial strains, including ATCC reference *Escherichia coli* and *Staphylococcus aureus* (*E. coli* and *S. aureus*), clinically isolated *Pseudomonas aeruginosa* (*P. aeruginosa*), as well as multidrug-resistant hard-to-treat methicillin-resistant *S. aureus* (MRSA) and extended spectrum  $\beta$ -lactamase *E. coli* (ESBL *E. coli*). The cytotoxicity profile has been evaluated using Balb/c 3T3 mouse fibroblasts via a direct contact assay, and Human dermal fibroblasts via an indirect (extract-based) assay. In the second stage, the antibacterial  $\epsilon$ -PL/HA hydrogel matrix has been functionalised with bioactive strontium-substituted hydroxyapatite (Sr-HAp) nanoparticles to develop antibacterial and bioactive injectable hydrogels for bone tissue regeneration. To evaluate application-specific performance, further physicochemical and biological characterisation has been performed, including sustained (up to 168 h) antibacterial activity against *E. coli*, *S. aureus*, MRSA, and ESBL *E. coli*.

The Doctoral Thesis has been elaborated as a summary of scientific articles. The summary of scientific articles is written in Latvian and English. It includes four scientific publications and one review article. Each summary contains 10 figures and one table, totalling 45 pages.

## USED ABBREVIATIONS

AMP	antimicrobial peptides
AMR	antimicrobial resistance
ATCC	American Type Culture Collection
Balb/c 3T3	fibroblast cells isolated from BALB/c mouse embryos
BSA	bovine serum albumin
CLSI	Clinical and Laboratory Standards Institute
CaP	calcium phosphates
CDC	Centers for Disease Control and Prevention
CRAB	carbapenem-resistant <i>Pseudomonas aeruginosa</i>
CRPA	carbapenem-resistant <i>Acinetobacter baumannii</i>
E'/'E''	compression storage/loss modulus
<i>E. coli</i>	<i>Escherichia coli</i>
ECM	extracellular matrix
EDC	1-ethyl-3-(3-dimethyl aminopropyl) carbodiimide
$\epsilon$ -PL	$\epsilon$ -polylysine
EPS	exopolysaccharides
ESBL	extended spectrum $\beta$ -lactamase producing bacteria strain
EU MDR	EU Medical Device Regulations
EUCAST	European Committee on Antimicrobial Susceptibility Testing
FDA	Food and Drug Administration
FTIR	Fourier transform infrared spectroscopy
G'/'G''	storage/loss modulus
GAG	glycosaminoglycans
GEN	gentamicin
HA	hyaluronic acid
HAp	hydroxyapatite
HCl	hydrochloric acid
HDF	human dermal fibroblasts
<i>in vitro</i>	experimental studies outside a living organism
LVR	linear viscoelastic region
<i>M. tuberculosis</i>	<i>Mycobacterium tuberculosis</i>
MBC	minimum bactericidal concentration
MIC	minimum inhibitory concentration
MRSA	methicillin-resistant <i>Staphylococcus aureus</i>

NaCl	sodium chloride
NaOH	sodium hydroxide
NDB	naturally derived biopolymer
aNDB	antibacterial naturally derived biopolymer
NHS	<i>N</i> -hydroxysuccinimide
<i>P. aeruginosa</i>	<i>Pseudomonas aeruginosa</i>
PRSP	penicillin-resistant <i>Streptococcus pneumoniae</i>
PVA	polyvinyl alcohol
RGD	arginine-glycine-aspartic acid
<i>S. aureus</i>	<i>Staphylococcus aureus</i>
<i>S. epidermidis</i>	<i>Staphylococcus epidermidis</i>
SAXS	small-angle X-ray scattering
SCI	scientific
SEM	scanning electron microscopy
Sr-HAp	strontium-substituted hydroxyapatite
USD	United States dollar
VAN	vancomycin
VRE	vancomycin-resistant <i>Enterococci</i>
WHO	World Health Organization

# TABLE OF CONTENTS

GENERAL DESCRIPTION OF THE RESEARCH.....	9
Introduction to the State-of-the-Art .....	9
Aim and Tasks .....	12
Thesis Statements to be Defended .....	13
Scientific Novelty .....	13
Practical Significance .....	13
Structure and Volume of the Doctoral Thesis .....	14
Publications and Approbation of the Doctoral Thesis.....	14
MAIN RESULTS OF THE DOCTORAL THESIS.....	18
Potential of Naturally Derived Biopolymers (NDBs) as Alternative Antibacterials for Tissue Engineering Applications (1st Publication).....	18
Development of a Novel Inherently Antibacterial Chemically Crosslinked Hydrogel Matrix (2nd Publication) .....	19
Optimisation of Synthesis Method, Evaluation of Topology and Impact of Steam Sterilisation on physicochemical and Antibacterial Properties of Chemically Crosslinked $\epsilon$ -PL/HA Hydrogels (3rd Publication) .....	24
<i>In Vitro</i> Evaluation of Antibacterial Potential and Cytotoxicity of $\epsilon$ -PL/HA Hydrogels (4th Publication) .....	29
Synthesis and Characterisation of Antibacterial Sr-HAp Functionalised $\epsilon$ -PL/HA Hydrogels (5th Publication) .....	33
CONCLUSIONS.....	37
REFERENCES.....	38

# GENERAL DESCRIPTION OF THE RESEARCH

## Introduction to the State-of-the-Art

According to data from the World Health Organization (WHO), bacterial infections account for 13.6 % of human mortality, equating to approximately one in every eight deaths worldwide [1]. The only widely used strategy for treating and preventing bacterial infections in healthcare remains antibiotics, with few non-antibiotic alternatives available, except for “last resort” bacteriophage therapy. Such “last resort” use is closely linked to the growing problem of antibiotic resistance among bacterial pathogens. The WHO and the Centers for Disease Control and Prevention (CDC) recognise antimicrobial resistance (AMR) as a global crisis due to the increased prevalence of pathogens resistant to last-resort antibiotics. For decades, a growing list of AMR-associated pathogens has been responsible for hundreds of thousands of deaths. These include penicillin-resistant *Streptococcus pneumoniae* (PRSP), carbapenem-resistant *Pseudomonas aeruginosa* and *Acinetobacter baumannii* (CRPA and CRAB), methicillin-resistant *Staphylococcus aureus* (MRSA), vancomycin-resistant *Enterococci* (VRE), and extended-spectrum  $\beta$ -lactamase (ESBL) producing *Escherichia coli* (*E. coli*). Moreover, it is estimated that by 2050, AMR-related deaths could exceed 10 million annually. To combat this growing crisis, the WHO Global Action Plan has underlined the urgent need to develop alternative non-antibiotic strategies [2].

Although naturally derived antibacterial biopolymers (aNDBs) [3]–[5] have long been used in biomedical applications, their study has expanded significantly in recent years. Unlike the others biopolymers that are used in biomedicine and could be both of natural (hyaluronic acid, gelatin etc.) and synthetic (polyvinyl alcohol (PVA), polyethylene glycol (PEG), etc.) origin, aNDBs are obtained from natural sources (plants, fungi, microorganisms, algae, and animals) and exhibit biocompatibility and intrinsic antibacterial activity without a need for additional chemical modifications [4]. Interest in aNDBs as non-antibiotic antibacterial agents has surged, with publications on their use increasing by nearly 400 % since 2015. This growing trend is primarily driven by recognising aNDBs as promising antibacterial molecules for local delivery applications, offering biocompatibility and antibacterial efficacy against pathogenic bacteria. Furthermore, it has been highlighted that bacteria are less likely to develop resistance against such material, as the antibacterial activity of aNDB differs from conventional antibiotics in both target specificity and mechanism of action [4]. Several studies have demonstrated the development of various biomaterials, such as drug delivery systems, ophthalmic contact lenses, injectable cements, medical device and implant coatings, microneedle patches, wound dressings, nanoparticles and nanofibers, and hydrogels based on aNDB with significant antibacterial activity [2], [6]–[8]. These aNDB include chitosan,  $\kappa$ -carrageenan, alginate, pectin, o-pullulan, fucoidan, chondroitin sulphate, bacterial-produced exopolysaccharides, as well as antimicrobial peptides (AMP) [2], [6]–[12].

Hydrogels have emerged as a promising class of biomaterials in biomedicine due to their high biocompatibility, tuneable mechanical properties, and ability to mimic the extracellular matrix (ECM) of human tissues. These properties make hydrogels particularly advantageous for tissue engineering and regenerative medicine, as they can support cell adhesion, proliferation, and differentiation, thereby promoting tissue regeneration. Over the past decade, research has increasingly focused on developing hydrogels with antibacterial functionality to

address the critical clinical challenge of infected tissue repair and healing. One of the most effective strategies involves the development of hydrogels based on aNDBs. These intrinsic antibacterial hydrogels offer several advantages, including eliminating additional antibacterial agents or antibiotics, a simplified composition, enhanced biocompatibility, and sustained antibacterial efficacy [13]. Beyond infection control, hydrogels are also being explored for applications in bone tissue regeneration. Bone defects and fractures resulting from diseases such as osteoporosis, osteosarcoma, and high-impact injuries represent a significant global health burden, affecting over 200 million people worldwide and incurring an economic cost exceeding \$100 million annually [14], [15]. These conditions are frequently complicated by a high risk of infection, especially in cases of open fractures, surgical interventions, and immunocompromised patients. Post-traumatic osteomyelitis, periprosthetic joint infections, and implant-associated infections remain significant clinical challenges, often leading to delayed bone healing, implant failure, and increased mortality rates. Consequently, developing multifunctional, bone-targeted antibacterial biomaterials with regenerative potential has become a key research focus to improve treatment outcomes and prevent infection-related complications in bone healing and regeneration.

A promising approach in this field involves the biofunctionalisation of the hydrogel matrix with bioactive and osteogenic inorganic components, such as calcium phosphate (CaP) particles. CaP bone biomaterials, such as hydroxyapatite (HAp), demonstrate excellent biocompatibility and bioactivity in physiological conditions, as they closely resemble the primary mineral component of bone extracellular matrix (ECM) [16], [17]. This similarity allows CaP-based biomaterials to form intimate functional interfaces with bone tissue, enhancing osseointegration and bone remodelling. However, despite their advantages, CaP biomaterials exhibit limitations such as low mechanical strength, uncertain biodegradation rate, and lack of cohesiveness. Moreover, commercially available bone biomaterials still fail to fully replicate the hierarchical composite structure of native bone tissue and exhibit limited regenerative potential for the treatment bone-related diseases [18]. Combining CaP with a hydrogel matrix enables the development of composite hydrogels with enhanced functionalities, including superior biocompatibility and bioactivity, improved structural integrity, optimised porosity, tuneable mechanical stiffness, and biodegradation rates. These properties make the composite hydrogel a promising biomaterial for bone regeneration, providing a bioactive and mechanically supportive environment for cell growth and tissue integration [17]. The current clinical gold standard for infected bone tissue treatment includes administration of systemic or local antibiotics, as well as a separate surgery to implant a bone graft for the reconstruction of bone tissue [19]. For local antibiotic therapy, synthetic poly (methyl methacrylate) (PMMA) bone cement beads and spacers are used to deliver a high concentration of antibiotics, for example, vancomycin (VAN), gentamicin (GENTA) [20]. However, bioinert non-biodegradable PMMA biomaterials as antibiotic carriers have substantial drawbacks, such as poor drug release kinetics [20], inducing the development of antibiotic resistance, providing a site for pathogen colonisation and biofilm formation, causing toxicity, and requiring additional surgery for removal. A one-step approach is demonstrated by bioactive GENTA or VAN loaded hydroxyapatite (HAp)/calcium sulphate biomaterials, a new commercially available injectable synthetic bone graft substitute, CERAMENT® G and CERAMENT® V (BONESUPPORT, Lund, Sweden). These commercial products have a significant advantage as they simultaneously provide local antibiotic therapy and promote new

bone formation [21]. However, local wound complications, persistent infection, and residual mature biofilm have been reported in treating chronic osteomyelitis. This is why naturally-derived CaP-loaded inherently antibacterial composite hydrogels are a tremendously important research direction to provide a potential solution for two common problems in the healthcare sector – bacterial infections and bone disorders. To address the AMR crisis and the challenges associated with bacterial infection treatment and bone reconstruction, the Doctoral Thesis focuses on the development and investigation of antibacterial hydrogels based on antimicrobial polypeptide  $\epsilon$ -polylysine ( $\epsilon$ -PL) and biologically active hyaluronic acid (HA), and  $\epsilon$ -PL/HA composite hydrogels.  $\epsilon$ -PL/HA composite hydrogels have been developed by functionalising the antibacterial hydrogel matrix with bioactive Sr-HAp nanoparticles. This approach aims to introduce specialised functional properties, such as supporting mesenchymal stem cell differentiation, influencing ECM protein adsorption, and enhancing cell adhesion and tissue formation, while mimicking the nanostructure and composition of native bone tissue to improve bone regeneration capability.

Firstly, the most important parameters in designing antibacterial hydrogels include the selection of suitable components and an appropriate crosslinking strategy. In this study,  $\epsilon$ -PL and HA have been selected based on the superior functional properties, providing both antibacterial activity and the ability to mimic the native ECM. HA is an essential polysaccharide of the ECM in many tissues, which demonstrates excellent biocompatibility and plays an important biochemical role in different physiological processes [22], [23]. Moreover, HA contains multiple functional groups that allow for numerous subsequent chemical modifications [13], [24]. Among typical short-chain antimicrobial peptides (AMPs),  $\epsilon$ -PL is classified as a long-chain antimicrobial polypeptide, also known as a poly(amino acid).  $\epsilon$ -PL has many unique characteristics and is generally recognised as safe by the Food and Drug Administration (FDA). It has several advantages compared to other AMPs, including natural origin, simple structure, low immunogenicity, low toxicity profile, biocompatibility, antibacterial mechanism through membrane disruption, stability under a range of pH and temperature, and cost-effectiveness. Until now, only a few studies have addressed the preparation and antibacterial evaluation of antibacterial hydrogels containing  $\epsilon$ -PL, including chemically crosslinked polyglutamic acid/ $\epsilon$ -PL composite hydrogels, bovine serum albumin (BSA) and polyvinyl alcohol (PVA) dual-network hydrogels with embedded  $\epsilon$ -PL, photo crosslinkable silk fibroin/ $\epsilon$ -PL hydrogels, polyacrylamide, gelatin, and  $\epsilon$ -PL hydrogels,  $\epsilon$ -PL-stabilized agarose/polydopamine hydrogels and dynamic arginine-glycine-aspartic acid (RGD)/  $\epsilon$ -PL hydrogels [2], [24].

To preserve properties of both components while combining them into a single integral hydrogel matrix, a chemical crosslinking approach using 1-ethyl-3-(3-dimethylaminopropyl) carbodiimide (EDC) and *N*-hydroxysuccinimide (NHS) has been selected. EDC/NHS crosslinking offers mild reaction conditions, water solubility of both reagents, lower toxicity compared to conventional crosslinkers, and improved mechanical properties of the resulting hydrogel matrix due to the formation of stable covalent bonds [25].

Secondly, the development of composite hydrogels requires the selection of an appropriate and well-justified CaP derivative. The main inorganic component of the bone extracellular matrix (ECM) is nanosized carbonated calcium-deficient apatite containing trace elements such as Mg, Zn, Sr, etc. Synthetic hydroxyapatite (HAp) nanoparticles have similarities to bone apatite in terms of chemical composition, structure, and size. Therefore, synthetic nanocrystalline HAp exhibits excellent osteoconductive properties. Various HAp-based

biomaterials have been extensively explored as carriers for the delivery of biologically active compounds due to their high specific surface area, unique bioactivity, and adsorption capacity across biological barriers [26]. Recently, HAp-based carriers for targeted delivery of antiosteoporotic drugs, anticancer drugs, antibiotics, proteins, genes, radionuclides, and inorganic ions, such as  $Mg^{2+}$ ,  $Zn^{2+}$ , and  $Sr^{2+}$ , have been investigated. Ion-substituted HAp biomaterials are considered advantageous systems for the sustainable, local delivery of the biomimetic bone ECM trace elements [27]–[29]. These functionalised HAp can be applied for developing next-generation biomaterials to treat and reconstruct bone disorders (including osteoporotic bone fractures) through the controlled delivery of biologically active inorganic ions or drugs directly to bone defect sites [30]. Among different candidates for the development of ion-substituted HAp,  $Sr^{2+}$  ions have been of wide interest since they act as a bone therapeutic agent by a unique dual-acting mechanism, that is, simultaneously promoting bone formation by activating Ca-sensing receptors and inhibiting bone resorption [31], [32].  $Sr^{2+}$  ions are incorporated into bone by two main mechanisms: (1) a rapid uptake mechanism dependent on osteoblast activity, whereby  $Sr^{2+}$  ions are absorbed via ion exchange processes with  $Ca^{2+}$  ions or binding to osteoid proteins, and (2)  $Sr^{2+}$  ions are incorporated into the crystal lattice of the bone mineral.  $Sr^{2+}$  ions have osteogenic potential, and it has been reported that Sr-containing HAp biomaterials can deliver  $Sr^{2+}$  ions to the site of a bone defect, where they assist in bone regeneration by promoting osteoblasts' proliferation and differentiation and suppressing osteoclast activity.

Considering the demonstrated potential of the selected components and crosslinking strategy, the Doctoral Thesis focuses on the development and comprehensive characterisation of injectable hydrogels combining the inherent antibacterial properties of  $\epsilon$ -PL, the ECM-mimicking and biocompatible properties of HA, and the osteogenic effect of Sr-HAp nanoparticles. This multifunctional hydrogel system has been designed to simultaneously combat bacterial infections and support bone tissue regeneration, addressing the abovementioned critical healthcare challenges.

## Aim and Tasks

The aim of the Doctoral Thesis is to use antimicrobial polypeptide  $\epsilon$ -PL to develop covalently crosslinked antibacterial hydrogels for tissue engineering applications. To achieve the set aim, the experimental plan of the Doctoral Thesis has been divided into four parts related to the synthesis methodology development of the hydrogels and Sr-HAp functionalised hydrogels and their further investigation. These parts correspond to the tasks set up in the Doctoral Thesis:

1. to develop a synthesis methodology of the chemically crosslinked  $\epsilon$ -PL/HA hydrogel matrix via EDC/NHS crosslinking agent-mediated reaction;
2. to investigate physicochemical and *in vitro* biological properties of prepared  $\epsilon$ -PL/HA hydrogels;
3. to develop a synthesis methodology of Sr-HAp nanoparticles functionalised  $\epsilon$ -PL/HA (Sr-HAp/ $\epsilon$ -PL/HA) hydrogels;
4. to investigate physicochemical and *in vitro* biological properties of the prepared Sr-HAp/ $\epsilon$ -PL/HA composite hydrogels.

## Thesis Statements to be Defended

1. An EDC/NHS-mediated chemical crosslinking approach has been used for the development of  $\epsilon$ -PL/HA hydrogels, enabling key physicochemical and biological properties relevant to tissue engineering applications, including stiffness, injectability, syringeability, self-recovery, sterilisation ability, antibacterial activity, and cell viability.
2. Covalently crosslinked  $\epsilon$ -PL/HA hydrogels can be sterilised using conventional steam sterilisation with minimal impact on their physicochemical and *in vitro* antibacterial performance.
3.  $\epsilon$ -PL/HA hydrogels demonstrate potent antibacterial activity against both Gram-negative and Gram-positive bacterial strains, including ATCC reference strains and clinically isolated hard-to-treat multidrug-resistant bacterial strains.
4. Functionalisation of  $\epsilon$ -PL/HA hydrogel matrix with Sr-HAp nanoparticles preserves the initial hydrogel matrix properties, including injectability and antibacterial activity, while introducing a tuneable biodegradation profile essential for bone tissue regeneration applications.

## Scientific Novelty

1. For the first time, a biocompatible and antibacterial hydrogel matrix has been developed using a combination of two naturally derived biopolymers,  $\epsilon$ -PL and HA, via EDC/NHS-mediated chemical crosslinking.
2. The impact of steam sterilisation on physicochemical properties and *in vitro* antibacterial activity of the developed  $\epsilon$ -PL/HA hydrogels has been systematically evaluated, demonstrating minimal impact on their functional properties and potential for clinical translation.
3. The potential for bacterial resistance development against  $\epsilon$ -PL has been investigated using both ATCC reference and clinically isolated multidrug-resistant Gram-negative and Gram-positive bacterial strains.
4. Injectable  $\epsilon$ -PL/HA hydrogels functionalised with Sr-HAp nanoparticles have been developed and evaluated for their dual functionality – antibacterial activity and osteogenesis capacity, highlighting their potential for application in bone infection treatment.
5. The time-dependent antibacterial activity of the  $\epsilon$ -PL/HA hydrogels and Sr-HAp functionalised  $\epsilon$ -PL/HA hydrogels has been investigated over fast-acting (24 h) and sustained (168 h) durations against a wide spectrum of bacterial strains, confirming a prolonged and broad-spectrum antibacterial activity of the developed hydrogel systems.

## Practical Significance

Within the Doctoral Thesis, the following practical outcomes have been achieved.

1. A robust and reproducible fabrication methodology has been developed for injectable, antibacterial, and autoclavable hydrogels based on  $\epsilon$ -PL and HA, using EDC/NHS-mediated chemical crosslinking for biomedical applications.
2. Standardised operating protocols have been developed for the investigation of viscoelastic properties, *in vitro* antibacterial activity, and cytocompatibility of the prepared

hydrogels, including detailed post-synthesis sample preparation procedures and validation of testing reproducibility.

3. An *in situ* functionalisation strategy has been developed to produce Sr-HAp functionalised  $\epsilon$ -PL/HA hydrogels as dual-functionality biomaterials, combining antibacterial activity with osteogenic capacity for the treatment of infected bone defects.
4. The simplicity of synthesis, sterilisation and modification ability of the developed hydrogel matrix suggest a strong translational potential for targeted antibacterial therapy, next-generation implant coatings, drug delivery vehicles, or composite materials.

### **Structure and Volume of the Doctoral Thesis**

The Doctoral Thesis has been elaborated as a summary of scientific publications dedicated to research on the development and comprehensive investigation of chemically crosslinked  $\epsilon$ -PL/HA hydrogel matrix and Sr-HAp functionalised  $\epsilon$ -PL/HA hydrogels. The Thesis includes four original research publications, published in scientific (SCI) journals, and one review article.

### **Publications and Approbation of the Doctoral Thesis**

Results and achievements obtained within the Doctoral Thesis have been published in four original scientific publications. In addition, a review article has been published, covering a related topic of the Thesis. During the development period of the Doctoral Thesis, the main results have been presented at 16 international scientific conferences.

#### *SCI publications*

1. **Scegljovs, A.**, Skadins, I., Chitto, M., Kroica, J., Salma-Ancane, K. (2025). Failure or Future? Exploring Alternative Antibacterials: A Comparative Analysis of Antibiotics and Naturally-Derived Biopolymers. *Front. Microbiol.*, 16, 1526250. doi: 10.3389/fmicb.2025.1526250 (IF 4.5, Q1, CiteScore 8.5).  
**Contribution of A. Scegljovs (85/100 %):** Conceptualisation, Writing – original draft, Writing – review & editing.
2. Salma-Ancane, K., **Scegljovs, A.**, Tracuma, E., Wychowaniec, J. K., Aunina, K., Ramata-Stunda, A., Nikolajeva, V., Loca, D. (2022). Effect of Crosslinking Strategy on the Biological, Antibacterial and Physicochemical Performance of Hyaluronic Acid and  $\epsilon$ -Polylysine Based Hydrogels. *Int. J. Biol. Macromol.*, 208, 995–1008. <https://doi.org/10.1016/J.IJBIOMAC.2022.03.207> (IF 8.5, Q1, CiteScore 10.3).  
**Contribution of A. Scegljovs (35/100 %):** Methodology, Validation, Formal analysis, Investigation.
3. **Scegljovs, A.**, Wychowaniec, J. K., Skadins, I., Reinis, A., Edwards-Gayle, C. J. C., D'Este, M., Salma-Ancane, K. (2023). Effect of Steam Sterilisation on Physico-Chemical Properties of Antibacterial Covalently Cross-Linked  $\epsilon$ -Polylysine/Hyaluronic Acid Hydrogels. *Carbohydr. Polym. Technol. Appl.*, 6, 100363. <https://doi.org/10.1016/J.CARPTA.2023.100363> (IF 6.5, Q1, CiteScore 11.0).  
**Contribution of A. Scegljovs (70/100 %):** Methodology, Validation, Formal analysis, Investigation.

4. **Sceglovs, A.**, Siverino, C., Skadins, I., Pirsko, V., Sceglova, M., Kroica, J., Moriarty, F. T., Salma-Ancane, K. (2025). Injectable  $\epsilon$ -Polylysine/Hyaluronic Acid Hydrogels with Resistance-Preventing Antibacterial Activity for Treating Wound Infections. *ACS Appl. Bio Mater.*, 8 (11), 9916–9930. <https://doi.org/10.1021/acsabm.5c01252>.  
**Contribution of A. Sceglovs (75/100 %):** Conceptualisation, Writing – original draft, Visualisation, Methodology, Validation, Investigation, Writing – review & editing.
5. Rubina, A., **Sceglovs, A.**, Ramata-Stunda, A., Pugajeva, I., Boyd, A. R., Tumilovica, A., Stipniece, L., Salma-Ancane, K. (2024). Injectable Mineralized Sr-Hydroxyapatite Nanoparticles-Loaded  $\epsilon$ -Polylysine-Hyaluronic Acid Composite Hydrogels for Bone Regeneration. *Int. J. Biol. Macromol.*, 280, 135703. <https://doi.org/10.1016/j.ijbiomac.2024.135703> (IF 8.5, Q1, CiteScore 10.3).  
**Contribution of A. Sceglovs (35/100 %):** Writing – review & editing, Writing – original draft, Visualisation, Investigation, Formal analysis, Conceptualisation.

#### *Participation in scientific conferences*

1. **Sceglovs, A.**, Reinis, A., Salma-Ancane, K. (2021). Natural Biopolymer-Based Antibacterial Hydrogels for Tissue Engineering. *European Society for Biomaterials (ESB 2021)*, 5–9 September 2021. Virtual event, virtual poster presentation.
2. **Sceglovs, A.**, Reinis, A., Salma-Ancane, K. (2021). Synthesis and Characterization of Chemically Cross-Linked Hydrogels Based on  $\epsilon$ -Polylysine and Hyaluronic Acid. *Materials Science and Applied Chemistry conference of RTU (MSAC 2021)*, 22 October 2021. Virtual event, virtual poster presentation.
3. **Sceglovs, A.**, Siverino, C., Moriarty, F. T., Salma-Ancane, K. (2022). Covalently Bonded  $\epsilon$ -Polylysine/Hyaluronic Acid Hydrogels with Enhanced Antibacterial Action. *Scandinavian Society for Biomaterials Conference (ScSB 2022)*, 13–15 June 2022, Jurmala, Latvia. Poster presentation.
4. **Sceglovs, A.**, Siverino, C., Wychowaniec, J. K., Moriarty, F. T., 'Este, M. D., Salma-Ancane, K. (2022). Functional  $\epsilon$ -Polylysine/Hyaluronic Acid Hydrogels with Antibacterial Activity. *Tissue Engineering and Regenerative Medicine International Society Conference (TERMIS EU 22)*, 28 June–1 July 2022, Krakow, Poland. Poster presentation.
5. **Sceglovs, A.**, Salma-Ancane, K. (2022). Effect of Steam Sterilization Strategy on  $\epsilon$ -Polylysine/Hyaluronic Acid Hydrogel Properties. *European Society for Biomaterials (ESB 2022)*, 4–8 September 2022, Bordo, France. Poster presentation.
6. Rubina, A., Kreicberga, I., **Sceglovs, A.**, Salma-Ancane, K. (2022). Development of Functional Composite Hydrogels for Bone Regeneration. *European Society for Biomaterials (ESB 2022)*, 4–8 September 2022, Bordo, France. Poster presentation.
7. **Sceglovs, A.**, Salma-Ancane, K. Investigation of Impact of Steam Sterilization on  $\epsilon$ -Polylysine/Hyaluronic Acid Hydrogel Properties. *Materials Science and Applied Chemistry Conference of RTU (MSAC 2022)*, 21 October 2022, Riga, Latvia. Poster presentation.
8. Rubina, A., Kreicberga, I., **Sceglovs, A.**, Salma-Ancane, K. (2022). Development of Functional Composite Hydrogels for Bone Regeneration. *Materials Science and Applied*

- Chemistry Conference of RTU (MSAC 2022)*, 21 October 2022, Riga, Latvia. Poster presentation.
9. **Scegljovs, A.**, Skadins, I., Pirsko, V., Kroica, J., Salma-Ancane, K. (2023). Injectable Polypeptide-Based Hydrogels for Local Antibacterial Therapy. *European Society for Biomaterials (ESB 2023)*, 4–8 September 2023, Davos, Switzerland. Poster presentation.
  10. Rubina, A., Tumilovica, A., **Scegljovs, A.**, Stipniece, L., Salma-Ancane, K. (2023). Injectable Hyaluronic Acid/ $\epsilon$ -Polylysine Hydrogels Loaded with Strontium Hydroxyapatite Nanoparticles for Osteoporotic Bone Fracture Healing. *European Society for Biomaterials (ESB 2023)*, 4–8 September 2023, Davos, Switzerland. Poster presentation.
  11. **Scegljovs, A.**, Skadins, I., Pirsko, V., Kroica, J., Salma-Ancane, K. (2023). Revealing Physicochemical and Antibacterial Properties of Chemically Coupled  $\epsilon$ -Polylysine/Hyaluronic Acid Hydrogel. *Materials Science and Applied Chemistry Conference of RTU (MSAC 2023)*, 6 October 2023, Riga, Latvia. Oral presentation.
  12. Rubina, A., Tumilovica, A., **Scegljovs, A.**, Stipniece, L., Salma-Ancane, K. (2023). Injectable Nanoparticle-Hydrogel Composites for Bone Regeneration. *Materials Science and Applied Chemistry Conference of RTU (MSAC 2023)*, 6 October 2023, Riga, Latvia. Oral presentation.
  13. **Scegljovs, A.**, Skadins, I., Kroica, J., Salma-Ancane, K. (2024). Injectable Hydrogels Based on Antimicrobial Polypeptide Exhibit Enhanced In Vitro Antibacterial Activity. *4th International Biennial BioMaH Conference*, 15–18 October 2024, Rome, Italy. Poster presentation.
  14. Rubina, A., **Scegljovs, A.**, Ramat-Stunda, A., Tumilovica, A., Stipniece, L., Salma-Ancane, K. (2024). Injectable Mineralized Sr-Hydroxyapatite Nanoparticles-Loaded Composite Hydrogels for Bone Regeneration. *4th International Biennial BioMaH Conference*, 15–18 October 2024, Rome, Italy. Oral presentation.
  15. **Scegljovs, A.**, Skadins, I., Kroica, J., Salma-Ancane, K. (2025). Advanced Hydrogel Platforms: Cross-Linked Polypeptide for Non-Antibiotic Antibacterial Applications. *RSU Research Week Biennial Conference (RW 2025)*, 24–28 March 2025, Riga, Latvia. Oral presentation.
  16. **Scegljovs, A.**, Rubina, A., Skadins, I., Wychowaniec, J. K., Ramat-Stunda, A., Kroica, J., Salma-Ancane, K. Attaining Non-Antibiotic Antibacterial Hydrogels: From  $\epsilon$ -Polylysine Networks to Composite Platforms. *Tissue Engineering and Regenerative Medicine International Society Conference (TERMIS EU 25)*, 19–23 May 2025, Freiburg, Germany. Oral presentation.

*Other scientific publications developed within the Doctoral Thesis*

1. Mosina, M., Severino, C., Stipniece, L., **Scegljovs, A.**, Vasiljevs, R., Moriarty, F. T., Locs, J. (2023). Gallium-Doped Hydroxyapatite Shows Antibacterial Activity against *Pseudomonas Aeruginosa* without Affecting Cell Metabolic Activity. *J. Funct Biomater.*, 14 (51). <https://doi.org/10.3390/jfb14020051>.
2. Stipniece, L., Ramata-Stunda, A., Vecstaudza, J., Kreicberga, I., Livkisa, D., Rubina, A., **Scegljovs, A.**, Salma-Ancane, K. (2023). A Comparative Study on Physicochemical Properties and In Vitro Biocompatibility of Sr-Substituted and Sr Ranelate-Loaded

- Hydroxyapatite Nanoparticles. *ACS Appl. Bio Mater.*, 6, 5264–5281. <https://doi.org/10.1021/acsabm.3c00539>.
3. Rubina, A., Tumilovica, A., **Sceglavs, A.**, Klavins, K., Vaska, A., Stipniece, L., Sizovs, A., Novosjolova, I., Salma-Ancane, K. (2025). Injectable Hyaluronic Acid/Nanohydroxyapatite Composite Hydrogels for Localized Drug Delivery and Bone Repair. *Carbohydr. Polym. Technol. Appl.*, 12, 101030. <https://doi.org/10.1016/j.carpta.2025.101030> (IF 6.5, Q1, CiteScore 11.0).

*Scientific conference presentations contributed as part of the Doctoral Thesis*

1. Tumilovica, A., Rubina, A., **Sceglavs, A.**, Stipniece, L., Salma-Ancane, K. (2023). Development of Injectable Composite Hydrogels Containing Hydroxyapatite Nanoparticles and Hyaluronic Acid. *Materials Science and Applied Chemistry conference of RTU (MSAC 2023)*, 6 October 2023, Riga, Latvia. Poster presentation.
2. Tumilovica, A., Rubina, A., **Sceglavs, A.**, Klavins, K., Stipniece, L., Salma-Ancane, K. (2024). Development of Injectable Bioactive Composite Hydrogels for Bone Regeneration. *4th International Biennial BioMaH Conference*, 15–18 October 2024, Rome, Italy. Poster presentation.

# MAIN RESULTS OF THE DOCTORAL THESIS

## Potential of Naturally Derived Biopolymers (NDBs) as Alternative Antibacterials for Tissue Engineering Applications (1st Publication)

Bacterial infections have been a significant problem throughout human history. Although the development of antibiotics in the 20th century revolutionised the treatment of infections, it also initiated an ongoing evolutionary struggle against pathogenic microorganisms. As a side problem, the overuse and misuse of these lifesaving antibiotics have developed the top global public health crisis named antimicrobial resistance (AMR) occurring worldwide [33]. The dramatic report by WHO has shown that by 2050, antibiotic resistance could become as deadly as cancer and cause substantial economic damage if no action is taken [34]. The decreasing efficacy of antibiotics and the limited availability of alternative treatments underscore the urgent need for new classes of antibacterial therapeutics. Ideal alternatives should include mechanisms of action that lower the risk of resistance development.

In this context, **antibacterial naturally-derived biopolymers (aNDBs)** have attracted significant attention due to their unique antibacterial properties. Approximately two decades ago, aNDBs with intrinsic antibacterial activity were first proposed as alternatives to antibiotics for treating bacterial infections [35]. Today, aNDB-based strategies show potential for localized, non-antibiotic antibacterial applications that support the immune system and minimise impact on the natural microbiota. Such approaches could represent a sustainable innovation within modern healthcare.

Regarding aNDBs, it is crucial to reveal their antibacterial mechanism against bacteria (Figure 1). Firstly, it is worth mentioning that bacterial cell wall outer structures (adhesion and pathogenicity factors), for example, lipopolysaccharides and phospholipids of Gram-negative bacteria and teichoic and lipoteichoic acids of Gram-positive bacteria, are negatively charged. Secondly, aNDBs consist of molecules (chondroitin sulphate,  $\alpha$ -pullulan,  $\epsilon$ -polylysine, chitosan, antimicrobial peptides, for example, magainin-2, etc.), which contain cationic groups like primary amines, quaternary ammonium, quaternary phosphonium, guanidinium or tertiary sulfonium [36], contributing to their overall positive charge at physiological pH. As a result, interaction between aNDB and bacteria begins with mutual attachment caused by electrostatic forces [37] (Figure 1). The electrostatic interaction represents the first step towards the bactericidal effect of aNDBs. Secondly, a specific concentration of cationicity of aNDBs must be achieved to reach a multivalence effect [38] that results in the simultaneous binding of aNDB molecules to the bacterial cell structures. Further mechanisms involve pore- or micelle-forming steps (Figure 1) that describe bacteria structural integrity disruption, leading to increased permeability, physical damages, and further entry into the cytoplasm and bacteria lysis.

Besides, several reports have shown that various aNDBs have antibiofilm activity as well. Antibiofilm mechanisms rely on mechanisms of disrupting biofilm exopolysaccharides (EPS), a crucial component for biofilm stability, leading to detachment of bacterial cells or preventing bacterial adhesion at the initial stage [39], [40]. In addition, different aNDBs, for example, lactoferrin-derived peptides, neutrophil peptides, antimicrobial peptides (protegrin-1), have been found to have antibacterial activity against intracellular bacteria – *M. tuberculosis*. Antibacterial mechanism is based on disrupting the mycobacterial cell wall and enhancing membrane permeabilization [9]–[11].

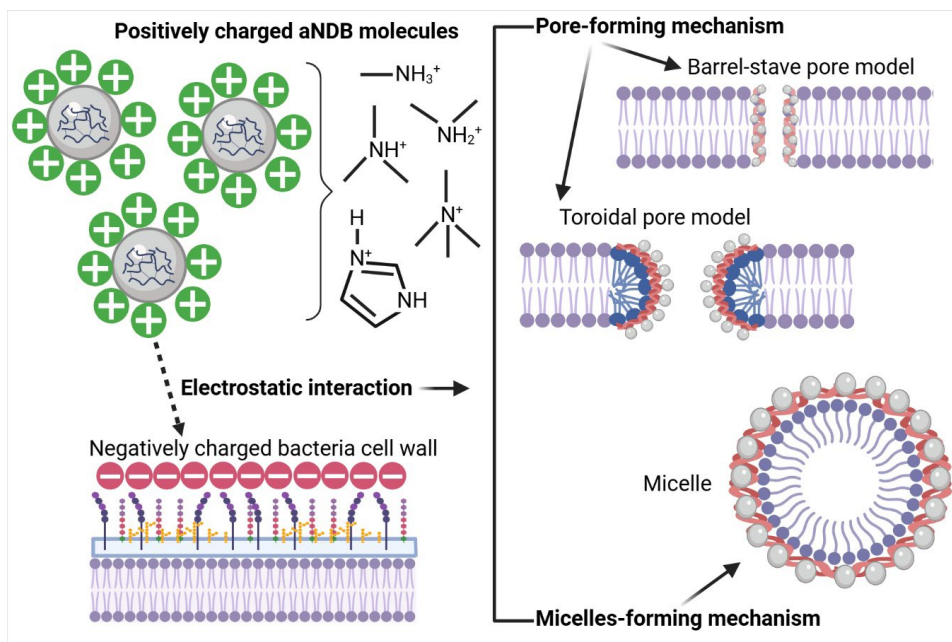


Figure 1. Biopolymer (aNDB) – bacteria cell interaction (left) and bactericidal mechanisms (right) (Created by Biorender).

Another crucial consideration is the potential for bacteria to develop resistance against aNDBs. Resistance mechanisms vary and are typically specific to the antibiotic class and its mode of action. Still, common mechanisms involve the production of specific enzymes, loss or modification of targeted molecules, activation of efflux pumps, mutations in the target sites, and alterations in cell permeability [12], [41]–[43]. It has been conventionally assumed that the development of resistance is exclusive to antibiotics, and that, theoretically, bacteria cannot develop resistance against aNDBs. On the one hand, electrostatic attraction between aNDB and bacterial outer structures seems inevitable. In addition, the aNDBs mechanism of action is not explicitly targeted. Even after penetrating the intracellular environment, aNDBs may interfere with multiple metabolic pathways [44]–[46]. Consequently, it is strongly believed that bacteria encounter challenges in impeding electrostatic interaction and developing resistance, given the biological expense associated with such a complex process.

## Development of a Novel Inherently Antibacterial Chemically Crosslinked Hydrogel Matrix (2nd Publication)

Hydrogels are innovative biomaterials for tissue engineering, regenerative medicine, and drug delivery applications due to their unique characteristics, such as the ability to encapsulate and release on demand the bioactive compounds (for example, drugs or growth factors) as well as support the cell proliferation and growth [47]–[49]. In recent years, particularly aNDB-based hydrogels with inherent antibacterial activity have been investigated as promising non-antibiotic antibacterial therapeutics for infection treatment in various biomedical applications such as wound healing and tissue infection prevention [24], [50], [51]. Among short-chain antimicrobial peptides (AMP), long-chain antimicrobial polypeptides or poly(amino acids)

such as  **$\epsilon$ -polylysine ( $\epsilon$ -PL)** have been spotlighted as a high-performance aNDB for antimicrobial biomaterial development [2], [52]–[54].  $\epsilon$ -PL is a naturally occurring, linear cationic antimicrobial polypeptide produced by *Streptomyces albulus*, classified as Generally Recognised as Safe (GRAS No. 000135) by the U.S. Food and Drug Administration, and provides broad-spectrum antimicrobial activity against both Gram-positive and Gram-negative bacteria. Besides its antibacterial mechanism via membrane disruption,  $\epsilon$ -PL has several advantages compared to other aNDBs, including a high abundance of free  $\epsilon$ -amino groups ( $-\text{NH}_2$ ), simple structure, low immunogenicity, low toxicity profile, ease of production and cost-effectiveness [2], [45], [55]–[57]. Until now, only a few studies have addressed the preparation and antibacterial evaluation of  $\epsilon$ -PL-based antibacterial hydrogels. Conversely, **hyaluronic acid (HA)** is an anionic and non-sulphated glycosaminoglycan (GAG) with unique physicochemical properties and distinctive biological functions. As a critical component of the native extracellular matrix (ECM), HA is an attractive building block for designing biomimetic, cell-interactive hydrogels for tissue bioengineering applications [58]–[60]. Hydrogels are mainly fabricated using a physical or chemical crosslinking approach or combining both methods to build 3D crosslinked polymer networks [61]. While possessing biomedical safety and ease of fabrication, physically crosslinked hydrogels present low mechanical properties and limited tuneable biodegradation due to the formation of reversible intermolecular interactions and weak secondary forces, such as ionic/electrostatic interaction, hydrogen bonding, etc. [61]–[63]. However, chemically crosslinked hydrogels are usually formed by chemically stable covalent crosslinking, resulting in better mechanical properties, stability in the physiological environment, and more tuneable biodegradation dynamics than the physically crosslinked hydrogels.

In the first part of the Doctoral Thesis, novel chemically crosslinked hydrogels based on  $\epsilon$ -PL and HA were prepared via water-soluble 1-ethyl-3-(3-dimethylaminopropyl) carbodiimide (EDC)/N-hydroxysuccinimide (NHS) mediated crosslinking between the carboxyl groups ( $-\text{COOH}$ ) of HA and the primary  $\epsilon$ -amino ( $-\text{NH}_2$ ) groups of  $\epsilon$ -PL, with constant EDC/NHS crosslinker concentration (1:1). The EDC/NHS concentration used in this study (0.24 M) was selected based on literature reports demonstrating its effectiveness in hydrogel crosslinking while maintaining non-cytotoxicity in cell culture applications [64]. Hydrogels were synthesized with varying  $\epsilon$ -PL to HA mass ratios of 40:60, 50:50 and 60:40 wt% to introduce the non-crosslinked primary amino groups of  $\epsilon$ -PL (Figure 2). As previously described, the non-crosslinked free amino groups of  $\epsilon$ -PL are primarily responsible for its antibacterial activity through electrostatic attachment to the bacterial outer surface. However, an excessively high concentration of free  $\epsilon$ -PL may increase the risk of cytotoxicity. Therefore, the main design concept was to combine antimicrobial polypeptide  $\epsilon$ -PL with biologically active HA to develop a covalently crosslinked hydrogel matrix that ensures not only structural stability, robust mechanical properties, and viscoelastic features, but also inherent antibacterial activity while maintaining cell viability [24]. To prevent premature gelation and to ensure efficient EDC/NHS-mediated crosslinking, all reagents were pre-cooled to 0–4 °C prior to the synthesis reaction (Figure 2).

The initial results on the physicochemical properties, *in vitro* cytotoxicity, and antibacterial activity of the developed  $\epsilon$ -PL/HA hydrogels were published in the collaborative study by Salma-Ancane et al. (2022) [24]. The aim of this study was to investigate the impact of varying  $\epsilon$ -PL mass ratios in  $\epsilon$ -PL/HA hydrogels on their physicochemical (Figure 3) and *in vitro*

biological properties. This included antibacterial activity against Gram-negative bacteria *E. coli* MSCL 332 (Figure 4A), as well as direct contact cytotoxicity assay to assess the cytotoxicity profile (IC<sub>50</sub>) of pure ε-PL towards the Balb/c 3T3 cell line (Figure 4B–C).

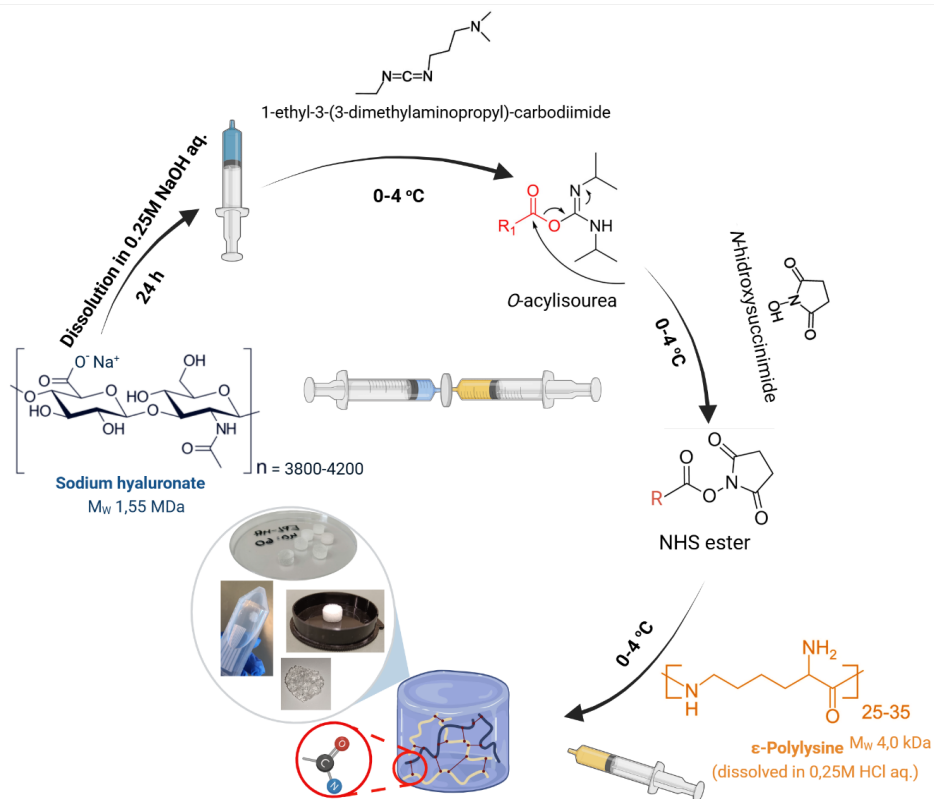


Figure 2. Schematic representation of the synthesis of chemically crosslinked ε-PL/HA hydrogels.

Physicochemical characterisation was performed to evaluate structural and functional properties (Figure 3A–D) of the developed chemically crosslinked ε-PL/HA hydrogels. X-ray diffraction (XRD) patterns (Figure 3A) revealed an amorphous structure of all prepared ε-PL/HA hydrogels with a characteristic amorphous diffraction maximum in the range of 2θ 20–23°. Additionally, diffraction peaks at 2θ 32°, 45° and 52° were observed and corresponded to the characteristic NaCl peaks. NaCl formed during the neutralisation reaction between salts of 0.25M NaOH and 0.25M HCl, in which synthesis was performed. Fourier transform infrared spectroscopy (FTIR) spectra (Figure 3B) of prepared ε-PL/HA hydrogels showed characteristic absorbance maximums that were found in pure components – ε-PL and HA. Thus, in FTIR spectra of prepared ε-PL/HA hydrogels, absorbance maximums at 1633 cm<sup>-1</sup>, 1555 cm<sup>-1</sup> and 1377 cm<sup>-1</sup> were referred to C=O stretching vibration (Amide I), C=O-NH bond vibration (Amide II), and C-N bond vibration (Amide III). Compared to the FTIR spectra of pure ε-PL and HA, slight shifts in the Amide I, Amide II and Amide III bands could be indicative evidence of chemical interaction between the free ε-amino groups of ε-PL and the carboxylic groups of HA, indicating the formation of covalent amide bonds during crosslinking. Furthermore, the calculated Amide I/Amide II ratio from normalised spectra of ε-PL/HA hydrogels and pure

component curves also revealed higher values of this ratio compared to pure  $\epsilon$ -PL, as the values of the three hydrogel compositions were found around 0.87, while the same band ratio for  $\epsilon$ -PL was 0.69. The absorption bands at 3246 and 3081  $\text{cm}^{-1}$  corresponded to unprotonated  $-\text{NH}_2$  and protonated  $-\text{NH}_3^+$  groups. As previously calculated, the  $\text{NH}_3^+/\text{NH}_2$  ratios of 0.65, 0.73 and 0.89 for the 40:60, 50:50 and 60:40 wt% compositions, respectively, indicate the presence of free  $\epsilon$ -amino groups of  $\epsilon$ -PL, which provide inherent antibacterial activity of the  $\epsilon$ -PL/HA hydrogels. Gel fraction test results (Figure 3C) showed similar values of gel content (51–57 %) with no statistically significant differences ( $p>0.05$ ), indicating a consistent crosslinking density across the prepared hydrogels. This consistency is attributed to the fixed HA content and constant molar concentrations of EDC and NHS used during synthesis.

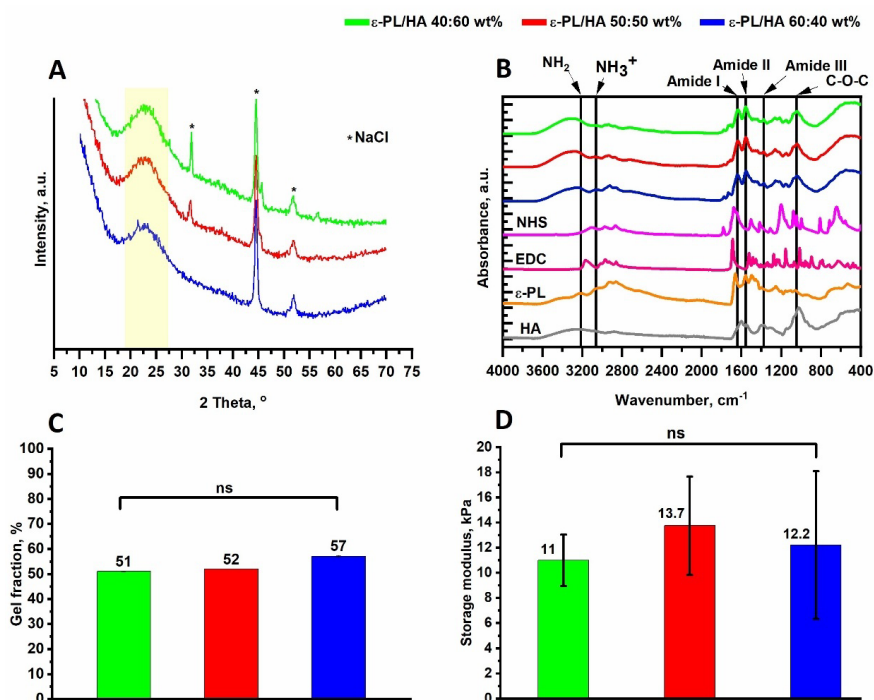


Figure 3. Summary of the main results from the investigation of the physicochemical properties of the  $\epsilon$ -PL/HA hydrogels [24]. (A) X-ray powder diffraction (XRD) patterns of the  $\epsilon$ -PL/HA hydrogels obtained in the  $2\theta$  range from 10 to 70. (B) Fourier transform infrared spectroscopy (FTIR) spectra of the  $\epsilon$ -PL/HA hydrogels and the pure components used in their preparation -  $\epsilon$ -PL, HA, EDC and NHS – recorded in a range of 400–4000  $\text{cm}^{-1}$ . (C) Gel fraction values for three different  $\epsilon$ -PL/HA hydrogel compositions presented as a bar chart (mean  $\pm$  SD). (D) Mechanical stiffness of the  $\epsilon$ -PL/HA hydrogel compositions, extracted from amplitude sweep curves at 1 Hz and 0.2 strain%. Three replicates were used from each experimental group.

From the *in vitro* evaluation of antibacterial activity, it was revealed that the chemically crosslinked  $\epsilon$ -PL/HA hydrogels exhibited antibacterial effect against the Gram-negative *E. coli* MSCL 332 (Figure 4A). Antibacterial activity was evaluated using both zone of inhibition test (24 h exposure) and the broth dilution test (1 h exposure), suggesting a rapid antibacterial effect upon direct contact and the release of a certain amount of free uncrosslinked  $\epsilon$ -PL molecules

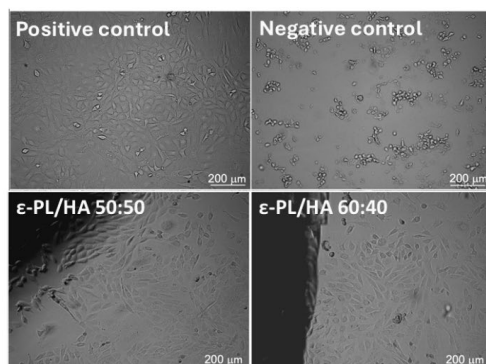
into the agar medium, as observed in the diffusion study. Furthermore, *in vitro* direct cell studies showed sustained cell viability and cell confluence after 24 h exposure (Figure 4B–C).

**A**

Designation	Diameter of inhibitory zone* $\pm$ SD [mm]	Log10 bacterial reduction**
$\epsilon$ -PL/HA 40:60 wt%	11.5 $\pm$ 0.6	1.8
$\epsilon$ -PL/HA 50:50 wt%	13.0 $\pm$ 1.2	2.7
$\epsilon$ -PL/HA 60:40 wt%	15.0 $\pm$ 0.0	3.3
Gentamicin, 10 mg/mL	30.7 $\pm$ 0.6	-

\* Zone inhibition test for 24 h against *E.coli* MSCL 332  
 \*\* Broth dilution test for 1 h against *E.coli* MSCL 332

**B**



**C**

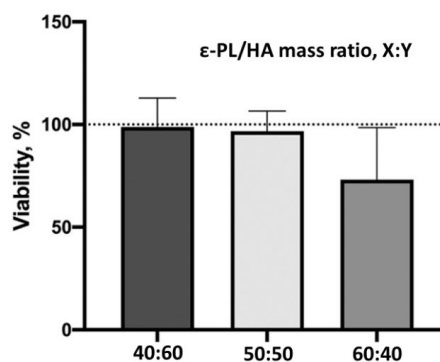


Figure 4. (A) Quantitative results from zone of inhibition test (24 h exposure) and broth dilution test (1 h exposure) against Gram-negative *E. coli* MSCL 332. (B) Microscopic images showing cell viability after 24 h of direct contact with the BALB/c 3T3 cell line. (C) Quantitative results on cell viability (expressed as %) for the prepared  $\epsilon$ -PL/HA hydrogel compositions after 24 h of direct contact with BALB/c 3T3 cells (right).

The first part of the Doctoral Thesis demonstrated that *in situ*-forming, chemically crosslinked  $\epsilon$ -PL/HA hydrogels can be successfully synthesized using an EDC/NHS-mediated polymerisation mechanism. The formation of new covalent bonds between  $\epsilon$ -PL and HA was revealed from molecular structure analysis by characteristic FTIR spectra comparing absorbance peaks, band shifts and intensity ratios of Amide I, Amide II and Amide III regions relative to the spectra of pure components. The calculated  $\text{NH}_3^+/\text{NH}_2$  ratios increased with higher  $\epsilon$ -PL content in the hydrogels, indicating a higher presence of protonated  $\epsilon$ -amino groups, which are associated with antibacterial activity. This trend was further supported by antibacterial assays. The cytotoxicity profile of pure  $\epsilon$ -PL showed an  $\text{IC}_{50}$  concentration at 4.21 mg/mL, indicating potential cytotoxicity effects at higher concentrations. However, all three hydrogel compositions demonstrated no cytotoxicity effect from direct exposure to BALB/c 3T3 cell lines from direct exposure to BALB/c 3T3 cell lines, highlighting the safety of the developed hydrogel systems. Chemical crosslinking was found to be an advantageous strategy, resulting in  $\epsilon$ -PL/HA hydrogels with enhanced structural integrity and a stable stiffness modulus in the range of 10–15 kPa, which is appropriate for musculoskeletal regeneration applications (Figure 3D) [63]. The stable covalent network also contributed to a

sustained antibacterial effect while maintaining low cytotoxicity. Furthermore, the preliminary results indicated that the chemically crosslinked  $\epsilon$ -PL/HA hydrogels could be sterilised by steam sterilisation (at 121 °C for 20 min) without compromising mechanical integrity.

In the second part of the Doctoral Thesis, the following research tasks were implemented: (a) synthesis optimisation to reduce the risk of HA degradation; (b) optimisation of the  $\epsilon$ -PL to HA mass ratio to achieve optimal mechanical features, high antibacterial activity, while ensuring cell viability; (c) evaluation of the hydrogels topology; (d) evaluation of the hydrogels viscoelastic properties; (e) investigation of the impact of steam sterilisation on physicochemical characteristics; and (f) assessment of *in vitro* antibacterial activity and cell viability.

### **Optimisation of Synthesis Method, Evaluation of Topology and Impact of Steam Sterilisation on physicochemical and Antibacterial Properties of Chemically Crosslinked $\epsilon$ -PL/HA Hydrogels (3rd Publication)**

First, the *in situ* forming method for synthesizing  $\epsilon$ -PL/HA hydrogels via EDC/NHS-mediated carboxyl-to-amine crosslinking was modified by using deionized water instead of 0.25M NaOH aq. (for HA) and 0.25M HCl aq. (for  $\epsilon$ -PL) (Figure 2). This modification aimed to prevent the risk of HA degradation under alkaline conditions during synthesis. In addition, the experimental design was expanded, and  $\epsilon$ -PL/HA hydrogels with  $\epsilon$ -PL to HA mass ratios of 40:60, 50:50, 60:40, 70:30 and 80:20 wt% were prepared.

Secondly, small-angle X-ray scattering (SAXS) analysis was performed to examine the internal structure and network topology of all of the fabricated hydrogels [13]. Topological features play a crucial role in their biomedical applications, as they influence viscoelastic behaviour, mechanical integrity, swelling, and biological interactions. Specifically, internal surface structure affects how biomaterial interfaces with living tissue, including cell adhesion, migration, mechanotransduction, proliferation, and antibacterial activity. SAXS analysis was performed over the  $q$ -range (0.045 nm<sup>-1</sup>–0.233 nm<sup>-1</sup>), corresponding to real-space dimensions of 27–140 nm. This range includes the Porod region of the hydrogel-like structures (of real  $d$  space), thus primarily providing information about the surface features and interface smoothness of the hydrogel network. The obtained scattering data were analysed using power-law fitting to extract the decay exponent ( $n$ ), which provides insight into surface topology. Results of the examined chemically crosslinked  $\epsilon$ -PL/HA hydrogels are presented as double logarithmic plots of  $q$ -decay (Figure 5A). A highly concentrated HA solution was used as the control, and exhibited decreased scattering intensity  $\sim q^{-3.9} \approx q^{-4}$ , indicating typical smooth surfaces formed by large polyelectrolyte complexes (Figure 5B) [65]. The chemically crosslinked  $\epsilon$ -PL/HA hydrogels showed similar decreased scattering intensities  $\sim q^{-3.6 \pm 0.4}$ , indicating smooth and robust network topologies, Porod surface (Figure 5B). This goes in line with the expected topological results for chemically crosslinked networks with smooth interfaces held by more robust covalent bonds. The exception,  $\epsilon$ -PL/HA hydrogel series with 40:60 wt% mass ratio, showed significantly different scattering intensity of  $\sim q^{-2.9}$  (Figure 5B), mostly typical of physically crosslinked aggregated clusters with rough interfaces [13]. As an outcome,  $\epsilon$ -PL/HA hydrogels with  $\epsilon$ -PL to HA mass ratios of 50:50, 60:40, 70:30 and 80:20 wt% were used in upcoming studies.

The ability of biomaterials, especially hydrogels, to withstand conventional steam sterilisation represents a significant advantage during early-stage development and clinical translation. Steam sterilisation is a highly effective, easily used and widely available sterilisation method. In the next step, the effect of steam sterilisation on the previously chosen hydrogel series was investigated to reveal in-depth physicochemical features. Then, topological evaluation was followed by scanning electron microscopy (SEM). SEM was used to observe the morphology of prepared freeze-dried hydrogel samples (Figure 5C). Both non-sterilised and sterilised samples showed a homogeneous three-dimensional network with interconnected porosity, with minimal effects visible for all hydrogels after sterilisation. Furthermore, pore size distribution after sterilisation for each ratio remained in a similar macroscale range of  $66.7 \pm 34.2 - 193.35 \pm 103.05 \mu\text{m}$ .

The gel fraction values for non-sterilised  $\epsilon$ -PL/HA hydrogel samples with  $\epsilon$ -PL to HA mass ratios of 50:50, 60:40, 70:30 and 80:20 wt%, were  $55.6 \pm 0.1$ ,  $56.2 \pm 0.2$ ,  $54.7 \pm 1.6$  and  $44.2 \pm 2.9\%$ , respectively (Figure 5D). These corresponded well to the first report values of  $\sim 55\%$  [24], except for the 80:20 wt% sample, which had significantly lower gel fraction. This lower value was ascribed to the lower extent of crosslinking for this ratio. Evidently, larger amounts of free, non-crosslinked  $\epsilon$ -PL were able to diffuse out during immersion in water, resulting in a decreased gel fraction, as a greater proportion of  $\epsilon$ -PL dissolved relative to the initial polymer mass in the hydrogel. No significant differences in gel fraction values were observed between non-sterilised and sterilised hydrogel samples within the same  $\epsilon$ -PL to HA mass ratio ( $p > 0.05$ ). This indicates that the steam sterilisation did not affect the overall extent of crosslinking in the  $\epsilon$ -PL/HA hydrogel samples, thereby preserving the network topology established during synthesis.

During swelling behaviour studies, both non-sterilised and sterilised  $\epsilon$ -PL/HA (ster  $\epsilon$ -PL/HA) hydrogels demonstrated swelling capability (swelling degree  $> 100\%$ ) after 2 h of incubation, and maintained plateau values over the entire study period (24 h, Figure 5E). In non-sterilised hydrogel samples, the swelling capacity increased with increasing  $\epsilon$ -PL mass ratio at 2 h, ranging from 116% for the 50:50 wt% composition to 340% for 80:20 wt% composition, respectively. For the 50:50, 60:40, and 80:20 wt% compositions, no significant differences were observed by 24 h ( $p > 0.05$ ). In contrast, the swelling capacity of ster  $\epsilon$ -PL/HA hydrogels with  $\epsilon$ -PL to HA mass ratio of 70:30 wt% increased from  $\sim 215\%$  to  $\sim 290\%$  ( $p < 0.05$ ), possibly indicating a reduction in mechanically active crosslinks. Despite this variation, all ster  $\epsilon$ -PL/HA hydrogels exhibited equilibrium swelling in the range of 116–350% (dependent on  $\epsilon$ -PL content), achieved after 4 h of incubation under physiological conditions (37 °C), demonstrating acceptable structural stability and cohesive properties for potential tissue engineering applications.

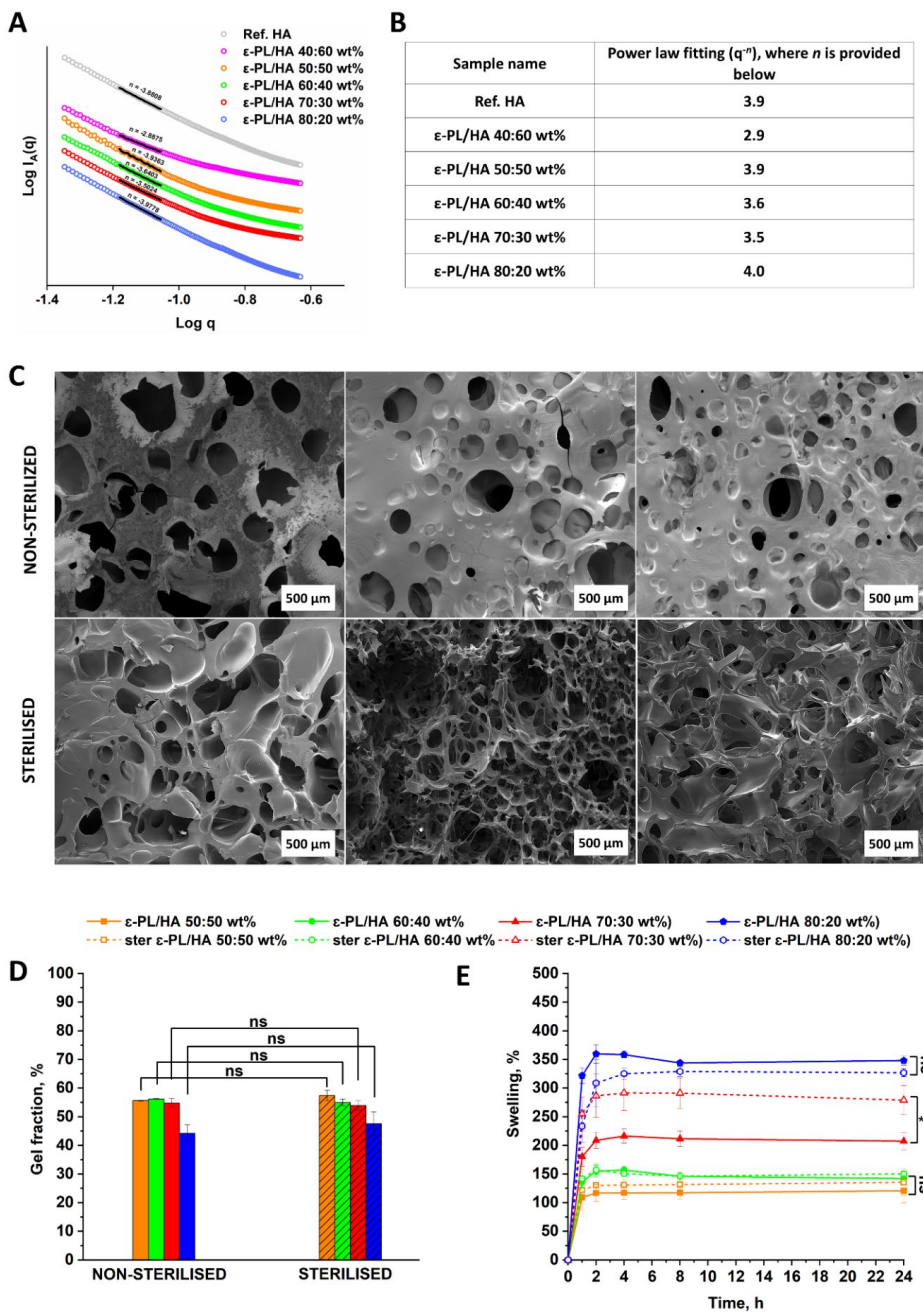


Figure 5. Investigation of the physicochemical properties of the  $\epsilon$ -PL/HA hydrogels [13]. (A) SAXS curves of the  $\epsilon$ -PL/HA hydrogels with mass ratios of 40:60, 50:50, 60:40, 70:30 and 80:20 wt%. (B) Calculated values of power law fitting index  $n$  from the  $q$ -decay ( $q^{-n}$ ). (C) SEM micrographs of non-sterilised (top) and sterilised (bottom) hydrogels; from left to right: 60:40, 70:30 and 80:20 wt%, respectively. (D) Gel fraction values of non-sterilised and sterilised  $\epsilon$ -PL/HA hydrogel samples. (E) Swelling behaviour curves of non-sterilised and sterilised samples. (D–E) Data are presented as mean  $\pm$  SD ( $n = 3$ ).

Various rheological studies were obtained to investigate the  $\epsilon$ -PL/HA hydrogel viscoelastic properties (Figure 6). Firstly, rheological features were observed as a function of hydrogel mass ratios and sterilisation. Amplitude sweep studies (Figure 6A–B) were performed in oscillation mode upon a strain range of 0.01 to 1000 strain% ( $\epsilon$ ), at a constant frequency of 1 Hz, equal to physiological conditions and 25 °C temperature. From the obtained curves of non-sterilised hydrogels (Figure 6A), it was concluded that hydrogels possessed soft solid-like behaviour with storage modulus ( $G'$ ) dominance prior to loss modulus ( $G''$ ) in the linear viscoelastic region (LVR). However,  $\epsilon$ -PL/HA hydrogels exhibited limited LVR in the range of  $\sim 0.1$ –1 % strain. In addition, observed  $G''$  behaviour with respect to  $G'$  showed the larger  $G'/G''$  ratio at lower strains but decreasing quite rapidly to a crossover point  $G' = G''$ . For all compositions, the crossover point remained as a  $\epsilon \approx 100$  %, highlighting hydrogel matrix resilience towards transition from solid to liquid mainly due to more stable and flexible chemical crosslinks. As for sterilised samples (Figure 6B), some minor differences were observed: (i) the crossover point ( $G'=G''$ ) of all compositions changed from previously identified  $\epsilon \approx 100$  % to  $\epsilon \approx 70$  %; (ii)  $G''$  behaviour at lower strain values ( $\sim 0.01$ –1 %) became identical for all the compositions compared with non-sterilised samples in the same strain value range. This could be explained as an outcome of sterilisation, resulting in partial loss of physical entanglements in the hydrogel matrix raised by uncrosslinked  $\epsilon$ -PL molecules and negatively charged HA functional groups. In the next step, storage modulus ( $G'$ ) values were extracted from amplitude sweep curves of both non-sterilised and sterilised hydrogel samples at  $\epsilon = 0.2$  % within the LVR (Figure 4C). Storage modulus values give insight into the mechanical stiffness of hydrogels. It was concluded that stiffness modulus for hydrogel compositions of 50:50, 60:40 and 80:20 wt% remained statistically insignificantly different ( $p > 0.05$ ) before and after sterilisation. However, for 70:30 wt%, this difference was significant ( $p < 0.05$ ), indicating that sterilisation had a higher effect on hydrogel structure and topology. Despite this finding, stiffness of  $\epsilon$ -PL/HA hydrogel compositions of 50:50, 60:40 and 70:30 wt% before and after sterilisation remained around 10 kPa, while 80:20 wt% composition showed a lower stiffness value of 8.6 kPa before sterilisation and dropped to 6.9 kPa after treatment. To sum up, these stiffness values suggest these hydrogels, after sterilisation, still address stiffness requirements (5–15 kPa) towards, for example, combined antibacterial and musculoskeletal regeneration applications [24].

Further rheological investigation was performed in flow mode and aimed to assess the injectability features of prepared hydrogel samples. From shear rate-dependent viscosity curves (Figure 6D), it can be seen that in case of all prepared samples, viscosity rapidly drops down as a function of increasing shear rate. This tendency suggests that prepared hydrogels are shear-thinning and can possess injectability/printability features. To answer more precisely that question, in the next step, recovery cycle studies were performed. The recovery cycles are performed to simulate the shear rate stress caused during the extrusion from a syringe/needle and to observe matrix recovery through viscosity values (Figure 6E).

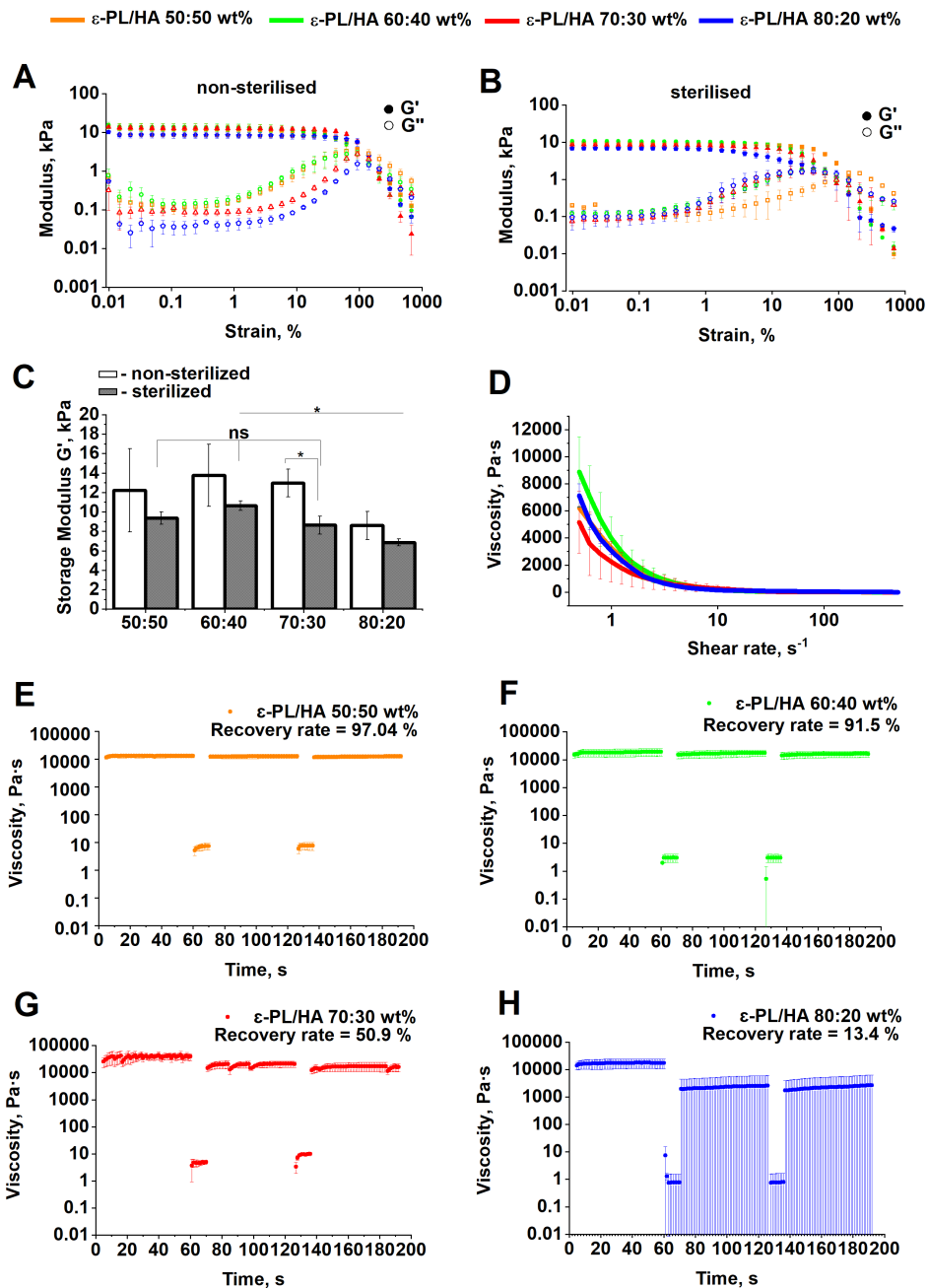


Figure 6. Rheological studies on prepared  $\epsilon$ -PL/HA hydrogels [2], [13]. (A–B) Amplitude sweep test curves of non-sterilised (A) and sterilised (B) hydrogel samples with different compositions. (C) Extracted storage modulus ( $G'$ ) from amplitude sweep at  $\epsilon = 0.2\%$  strain (LVR). (D) Shear rate-dependent viscosity graph. (E–H) Recovery cycle test performed over five cycles (3+2), comprising three stress-free cycles at a shear rate of  $0.1\ s^{-1}$  for 60 s, and 2 stress-induced cycles at  $200\ s^{-1}$  for 10 s. All rheological measurements were performed in triplicate to ensure reproducibility and data reliability.

Overall, the curves showed recovery features of broken intermolecular sites after induced stress conditions, that is, high shear rate values. It was found that compositions of 50:50 and 60:40 wt% were most suitable in terms of injectable biomaterials as they possessed a stable recovery rate higher than 90 % after multiple stress-induced cycles. Lower recovery values were found for 70:30 wt% composition, suggesting lower matrix integrity and flexible chain presence. However,  $\epsilon$ -PL/HA hydrogels with 80:20 wt% composition showed dramatically low recovery features, as only 13.4 % of the viscosity recovered compared to the initial viscosity values and possibly only due to the presence of a separate cluster in the broken hydrogel sample. As a result, three compositions of 50:50, 60:40 and 70:30 wt% were able to show recovery features. Possible difference of values between them can be explained again by structural integrity, as by increasing  $\epsilon$ -PL mass ratio, more uncrosslinked  $\epsilon$ -PL molecules interconnect with HA functional groups during synthesis, thereby interrupting chemical crosslinking network formation and organisation.

To sum up, physicochemical characterisation was performed for a series of  $\epsilon$ -PL/HA hydrogels with varying  $\epsilon$ -PL to HA mass ratios. The hydrogels showed gel fraction values, as well as swelling behaviour typical of hydrogels for tissue engineering applications. Furthermore, it was confirmed that the hydrogels could undergo steam sterilisation without significantly affecting these key properties. However, the rheological analysis revealed that 80:20 wt% composition did not meet the desired viscoelastic requirements for injectability and mechanical stiffness. Based on these findings, only 50:50, 60:40 and 70:30 wt%  $\epsilon$ -PL/HA hydrogel compositions were selected for further *in vitro* biological evaluation within the Doctoral Thesis.

### ***In Vitro* Evaluation of Antibacterial Potential and Cytotoxicity of $\epsilon$ -PL/HA Hydrogels (4th Publication)**

In the first part of the Doctoral Thesis, the preliminary studies confirmed the antibacterial potential of the developed  $\epsilon$ -PL/HA hydrogels against *E. coli* MSCL 332, using zone of inhibition and broth dilution assays at short (1 h) and extended (24 h) exposure times. However, firstly, it was crucial to investigate the antibacterial profile of pure  $\epsilon$ -PL by determining its minimum inhibitory and bactericidal concentrations (MIC/MBC), as well as assessing the potential for bacterial resistance development. The antibacterial activity of pure  $\epsilon$ -PL and  $\epsilon$ -PL/HA hydrogels was characterised by the broth dilution method via direct/indirect contact according to modified CLSI and EU CAST standards [66]. Antibacterial studies were performed against various Gram-negative and Gram-positive bacteria strains, including ATCC reference *Escherichia coli* (*E. coli*), *Staphylococcus aureus* (*S. aureus*) and *Staphylococcus epidermidis* (*S. epidermidis*), clinically isolated *Pseudomonas aeruginosa* (*P. aeruginosa*) and hard-to-treat clinically isolated multidrug-resistant Methicillin-resistant *Staphylococcus aureus* (MRSA), Extended spectrum  $\beta$ -lactamase *Escherichia coli* (ESBL *E. coli*) bacteria. MIC and MBC values of pure  $\epsilon$ -PL are presented in Table 1. Results showed inhibitory (MIC) and bactericidal (MBC) activity against all previously mentioned bacteria strains on a microgram scale, while IC50, as previously found, was 4.21 mg/mL on the mouse fibroblast cell line Balb/c 3T3. These results suggest that it is possible to moderate the  $\epsilon$ -PL mass ratio in hydrogel samples to achieve a high antibacterial activity while ensuring cell viability.

Table 1

The Obtained Values of MIC/MBC Concentrations of Pure $\epsilon$ -PL		
Bacterial strain	MIC of $\epsilon$ -PL, $\mu\text{g/mL}$	MBC of $\epsilon$ -PL, $\mu\text{g/mL}$
<i>E. coli</i>	37	75
<i>P. aeruginosa</i>	75	350
ESBL <i>E. coli</i>	18	37
<i>S. aureus</i>	37	75
<i>S. epidermidis</i>	18	37
MRSA	37	75

Furthermore, it was demonstrated that neither reference strains (*E. coli* and *S. aureus*) nor clinically isolated multidrug-resistant strains (ESBL *E. coli* and MRSA) developed resistance to  $\epsilon$ -PL over the experimental timeframe of 1 month (10 passages), highlighting the strong potential of  $\epsilon$ -PL/HA hydrogels for future antibacterial applications (Figure 7).

The results for  $\epsilon$ -PL/HA hydrogels demonstrated a statistically significant inhibition of bacterial colony growth after 24 h of contact ( $p < 0.05$ ) compared to control samples, across all tested bacterial strains and hydrogel compositions (Figure 8A). However, several key findings were observed: (i) the inhibition rate, presented as  $\text{Log}_{10}$  reduction, was dependent on the  $\epsilon$ -PL mass ratio in hydrogel compositions, that is,  $\epsilon$ -PL/HA of 70:30 wt% mass ratio showed the highest inhibition rate.

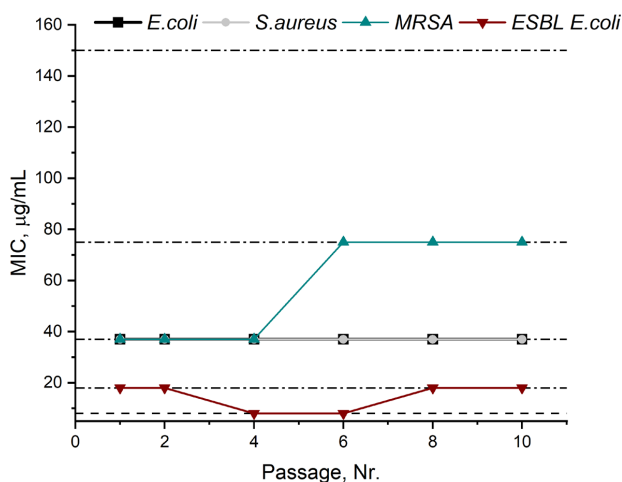


Figure 7. Bacterial resistance development studies of pure  $\epsilon$ -PL against *E. coli*, *S. aureus*, MRSA, and ESBL *E. coli* bacteria. The experiment was performed over 10 passages, with bacterial cultures re-cultivated from sub-MIC concentrations at each step.

In the case of *S. epidermidis*, *P. aeruginosa*, and MRSA, complete bacterial eradication was achieved; (ii) for the 50:50 and 60:40 wt% hydrogel compositions, a clear trend of efficient inhibition was observed against Gram-positive strains, including the reference *S. aureus* and *S. epidermidis*, as well as the clinically isolated multidrug-resistant MRSA. In contrast, a lower inhibition activity was achieved against Gram-negative strains (*E. coli*, *P. aeruginosa* and ESBL *E. coli*). This difference may be attributed to the unique structural features of Gram-

negative bacterial cell walls, such as the presence of an outer membrane that serves as an additional barrier to penetration of polypeptide molecules, and the action of efflux systems that can reduce intracellular accumulation of antibacterial agents.

The antibacterial potential of the  $\epsilon$ -PL/HA hydrogels over a sustained timeframe (up to 168 h) was investigated. The hydrogel samples were incubated for a week, with media refreshing cycles performed after 1 h and 24 h of incubation. This approach aimed to evaluate whether, following the initial rapid release of uncrosslinked  $\epsilon$ -PL, expected to occur within the first 24 h, the  $\epsilon$ -PL/HA hydrogel matrix could still provide a sustained release of  $\epsilon$ -PL due to gradual matrix degradation. After 168 h, both direct contact and indirect test (supernatant-based) antibacterial assays were performed using 24 h exposure against Gram-negative *E. coli* and Gram-positive *S. aureus* (Figure 8B). The results showed that all compositions of hydrogels retained a statistically significant antibacterial activity ( $p < 0.05$ ) through both exposure routes: direct bacteria contact with the hydrogel matrix and indirect contact with supernatants collected at 168 h. Notably, the 50:50 wt%  $\epsilon$ -PL/HA hydrogel composition exhibited the lowest inhibition rate compared to the other compositions in both exposure types against *S. aureus*, suggesting that its denser, and more compact matrix may have resulted in reduced degradation rate and limited availability of positively charged functional groups at the hydrogel surface.

Cytotoxicity was evaluated, using both direct and indirect contact approaches, (Figure 8C–D). In the indirect assay (Figure 8D), using Human Dermal Fibroblasts (HDFs), all  $\epsilon$ -PL/HA hydrogels formulations exhibited no cytotoxicity at extract concentrations up to 4.35 mg/mL, as cell viability remained above 70 % (the threshold for non-cytotoxicity defined by ISO 10993-5:2009 [67]) after 48 h of exposure. Notably, at an extract concentration of 2.025 mg/mL, cell viability was significantly higher than the control, suggesting that  $\epsilon$ -PL may promote cell proliferation when applied at appropriate concentrations. Interestingly, that 50:50 wt%  $\epsilon$ -PL/HA composition showed no cytotoxicity (cell viability > 70 %) toward HDFs at concentrations up to 93.023 mg/mL [2]. This finding aligns with results from the long-term antibacterial study, where the same composition exhibited lower antibacterial activity, possibly due to its denser and more compact crosslinking matrix, resulting in reduced  $\epsilon$ -PL release and lower surface charge. Furthermore, a cytotoxic effect was observed for the  $\epsilon$ -PL/HA 60:40 wt% composition at 20.12 mg/mL, while for the 70:30 wt% composition at as low as 9.36 mg/mL, indicating a correlation between increasing  $\epsilon$ -PL content in hydrogel samples and decreased cell viability. At concentrations  $\geq 93.023$  mg/mL, all compositions exhibited significant cytotoxicity [2]. Direct contact studies with Balb/c 3T3 cells (Figure 8C) after 24 h of exposure indicated mild cytotoxicity across all  $\epsilon$ -PL/HA hydrogel series, with cell viability remaining close to the acceptable threshold ( $\sim 70$  %),  $69.5 \pm 16.8$ ,  $65.3 \pm 17.4$ ,  $71.5 \pm 7.9$  for 50:50, 60:40, and 70:30 wt% hydrogel compositions, respectively. No statistically significant differences were observed between the compositions.

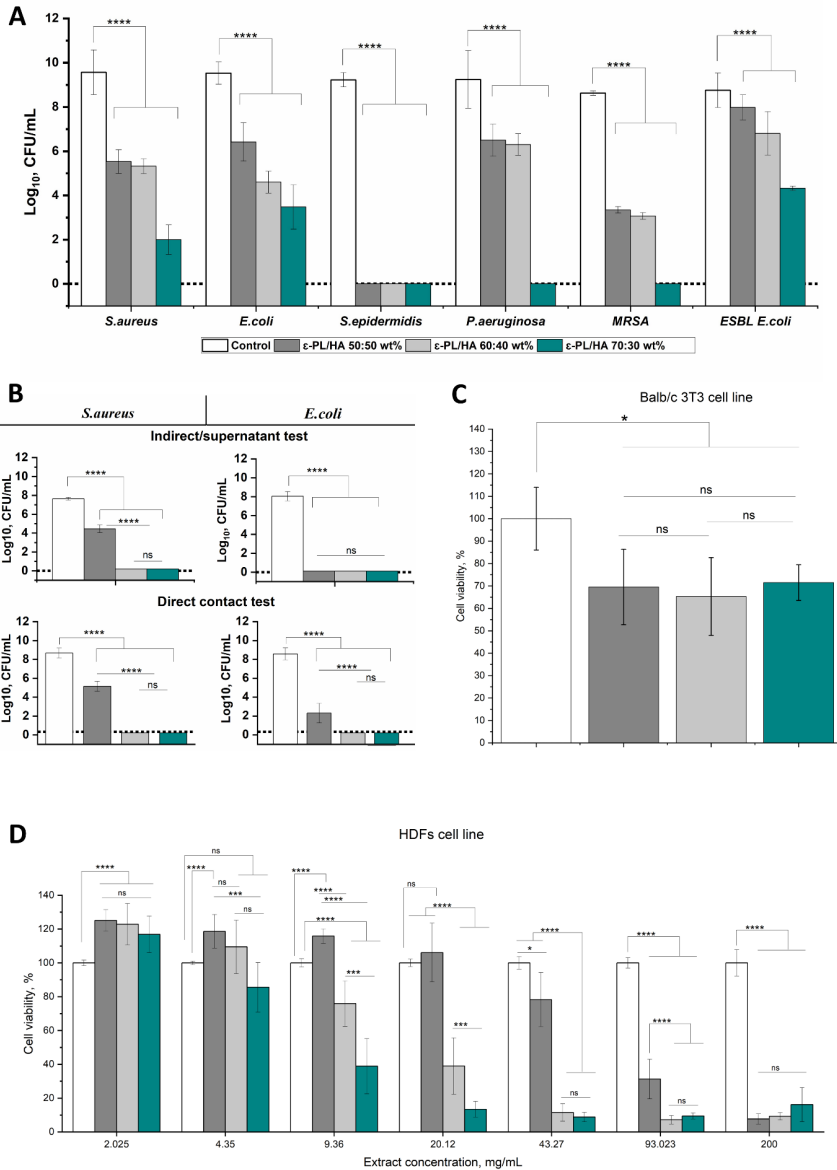


Figure 8. *In vitro* studies on prepared ε-PL/HA hydrogels [2]. A unified colour palette was used for all ε-PL/HA hydrogel compositions across the graphs and is provided as a legend below Graph A. (A) Direct contact studies using the broth dilution method against various Gram-negative and Gram-positive bacteria strains. Results of inhibition rate are presented as Log<sub>10</sub> reduction in bacterial count. (B) Direct contact and indirect (supernatant-based) antibacterial studies after 168 h incubation, with media refreshing at 1 h and 24 h, provided against *E. coli* and *S. aureus*. (C) Direct cell viability assay using the Balb/c cell line after 24 h exposure. (D) Indirect cell viability assay using the HDF cell line after 48 h exposure to various extract concentrations. Three replicates were used in each experiment, and results are presented as mean ± SD.

To summarise, the investigation of antibacterial properties showed inhibitory activity of the  $\epsilon$ -PL/HA hydrogels against a broad spectrum of Gram-positive and Gram-negative bacterial strains, including clinically relevant and multidrug-resistant bacteria. Furthermore, the *in vitro* indirect cytotoxicity assay (48 h) revealed dose-dependent of  $\epsilon$ -PL on cell viability. These findings clearly demonstrate that the both antibacterial activity and cell viability of the  $\epsilon$ -PL/HA hydrogels can be modulated by adjusting the  $\epsilon$ -PL concentration within the hydrogel matrix. Among the tested compositions, the  $\epsilon$ -PL/HA 50:50 wt% composition emerged as the most promising candidate, exhibiting a significant and sustained antibacterial activity across various bacterial strains, while maintaining acceptable cell viability, achieving a favourable balance between antibacterial performance and biocompatibility.

### **Synthesis and Characterisation of Antibacterial Sr-HAp Functionalised $\epsilon$ -PL/HA Hydrogels (5th Publication)**

Previously, the developed  $\epsilon$ -PL/HA hydrogel composition with a 50:50 wt% showed fast-acting (up to 24 h) and sustained (up to 168 h) an antibacterial activity against a broad spectrum of pathogens, while also demonstrating favourable cell viability, ability for steam sterilisation, injectability, and smooth surface topology. Based on these properties, the 50:50 wt%  $\epsilon$ -PL/HA hydrogel composition was selected for further development of the composite system by functionalisation of  $\epsilon$ -PL/HA hydrogel matrix with strontium-substituted hydroxyapatite (Sr-HAp) nanoparticles. This functionalisation aimed to unite the advantageous features of both components: the viscoelastic and inherent antibacterial properties of the developed  $\epsilon$ -PL/HA hydrogel matrix and the bone regeneration-promoting properties of Sr-HAp nanoparticles, toward the development of antibacterial and bioactive hydrogels for bone tissue engineering applications.

In this study, several compositions were developed, including a pure  $\epsilon$ -PL/HA hydrogel matrix with 50:50 wt% composition, and Sr-HAp/ $\epsilon$ -PL/HA composite hydrogels with varying inorganic (Sr-HAp): organic ( $\epsilon$ -PL/HA 50:50 wt%) mass ratios of 40 %, 50 % and 60 % (Figure 9A).

As injectability is an advantageous feature for biomaterials, particularly in bone regeneration applications, the injection force of the as-prepared hydrogels was investigated (Figure 9B). The results showed that all compositions, including the pure  $\epsilon$ -PL/HA hydrogel matrix, could be injected through a syringe with a tip inner diameter of 1.8 mm under an applied injection force of 3N. According to literature, needle gauge sizes ranging from 10 (inner diameter 2.69 mm) to 16 (inner diameter 1.19 mm) are considered suitable for orthopaedic procedures such as filling bone defects and cracks [68]. Additionally, the injection force should remain below 30 N, which is defined as the upper limit of manual injectability [69]. Based on this criteria, the developed hydrogels can be classified as manually injectable and suitable for potential clinical applications.

To investigate viscoelastic properties of the Sr-HAp/ $\epsilon$ -PL/HA hydrogels, compression studies were provided as part of their rheological characterisation. The compression test results (Figure 9C) revealed comparable behaviour across all tested compositions, with compression storage modulus ( $E'$ ) values of  $\sim 1000$  kPa within the physiological frequency range (0.1–10 Hz). According to the literature data, the compression storage modulus ( $E'$ ) values of composite platforms designed for bone tissue regeneration typically range from 100 kPa to

several MPa [70], [71]. Thus, the compression storage modulus values of the Sr-HAp/ $\epsilon$ -PL/HA hydrogels fall within the expected range for bone tissue regeneration applications. However, it should be noted that these studies do not provide a comprehensive evaluation of the mechanical properties, particularly under dynamic or load-bearing conditions. Therefore, Sr-HAp/ $\epsilon$ -PL/HA hydrogels cannot be considered suitable for load-bearing applications. However, they may still serve as promising biomaterials for providing favourable conditions for the natural bone remodelling process by maintaining nutrition transport, possessing porosity for cell migration, retaining structural integrity, and mimicking key features of the extracellular matrix [72].

To support the previously defined practical functionality, in further studies enzymatic degradation and kinetic profiles of ion release ( $\text{Ca}^{2+}$  and  $\text{Sr}^{2+}$ ) were performed. Enzymatic degradation curves (Figure 9D) showed that Sr-HAp/ $\epsilon$ -PL/HA degraded in hyaluronidase enzyme-containing PBS media over 20 weeks. While 0% Sr-HAp compositions showed a gradual degradation trend, reaching complete degradation after 20 weeks, the 40 %, 50 % and 60 % Sr-HAp compositions degraded more rapidly, achieving full degradation already after 5, 10 and 16 weeks, respectively. These results suggest that the biodegradation profile of Sr-HAp/ $\epsilon$ -PL/HA hydrogels is a function of Sr-HAp content and could be tuned to match specific application requirement in bone regeneration. Regarding ion release curves, it was observed that  $\text{Ca}^{2+}$  and  $\text{Sr}^{2+}$  ions were released in a burst manner when loaded into hydrogels compared with the pure Sr-HAp release profile (Figure 9E–F). A reason for that could lie in the acidic nature of the  $\epsilon$ -PL/HA hydrogel matrix, which could result in Sr-HAp dissolution, causing burst release observed within the first days of the experiments. Subsequently, the release of  $\text{Ca}^{2+}$  and  $\text{Sr}^{2+}$  ions from the Sr-HAp/ $\epsilon$ -PL/HA hydrogels proceeded in a slow and continuous manner over three months of the experimental period. Importantly, the concentration of  $\text{Sr}^{2+}$  ions did not exceed 20–30  $\mu\text{M}$ , while  $\text{Ca}^{2+}$  ions release ranged between 200 and 350  $\mu\text{M}$ . Previous studies have shown that  $\text{Sr}^{2+}$  ion concentrations up to 40  $\mu\text{M}$  are beneficial for the proliferation of osteoblasts in the cell culture [73], and the elevated  $\text{Ca}^{2+}$  ion concentration level up to 900  $\mu\text{M}$  can further enhance the bone regenerative effects of  $\text{Sr}^{2+}$  ions [73].

Finally, the antibacterial activity of the Sr-HAp/ $\epsilon$ -PL/HA hydrogels was evaluated in both rapid (24 h) and sustained (168 h) timeframes (Figure 10). Experimental time points were set as 24 h, 48 h, 72 h and 168 h, and studies were performed against Gram-positive bacteria: *S. aureus* (*Staphylococcus aureus*, ATCC 25923, reference), MRSA (methicillin-resistant *Staphylococcus aureus*, clinically isolated multidrug resistant strain), and Gram-negative bacteria: *E. coli* (*Escherichia coli*, ATCC 25922, reference), ESBL *E. coli* (extended spectrum  $\beta$ -lactamase *Escherichia coli*, clinically isolated multidrug-resistant strain). The obtained results revealed that experimental series of Sr-HAp/ $\epsilon$ -PL/HA hydrogels were able to inhibit both reference and clinically isolated multidrug-resistant Gram-negative and Gram-positive bacterial strains. However, several tendencies and subtleties must be highlighted. First of all, a higher inhibition rate was observed against Gram-positive bacteria, both reference and resistant strains. These results are in agreement with previous results on pure  $\epsilon$ -PL/HA hydrogels (Figure 8A) and were similarly re-observed in the case of 0% Sr-HAp. In general, a relatively high inhibition rate was maintained for all Sr-HAp/ $\epsilon$ -PL/HA hydrogel series throughout the entire experimental timeframe. Secondly, a sufficiently lower inhibition rate, compared to Gram-positive bacteria, was achieved against Gram-negative bacteria (both reference and clinical isolates). At the 24 h time point, the antibacterial activity of the 0% Sr-HAp composition closely matched previously obtained results for 50:50 wt%  $\epsilon$ -PL/HA hydrogel composition (Figure 8A). Furthermore, statistically significant inhibition of *E. coli* and ESBL *E. coli* was observed for all experimental series only under short-term conditions (24 h).

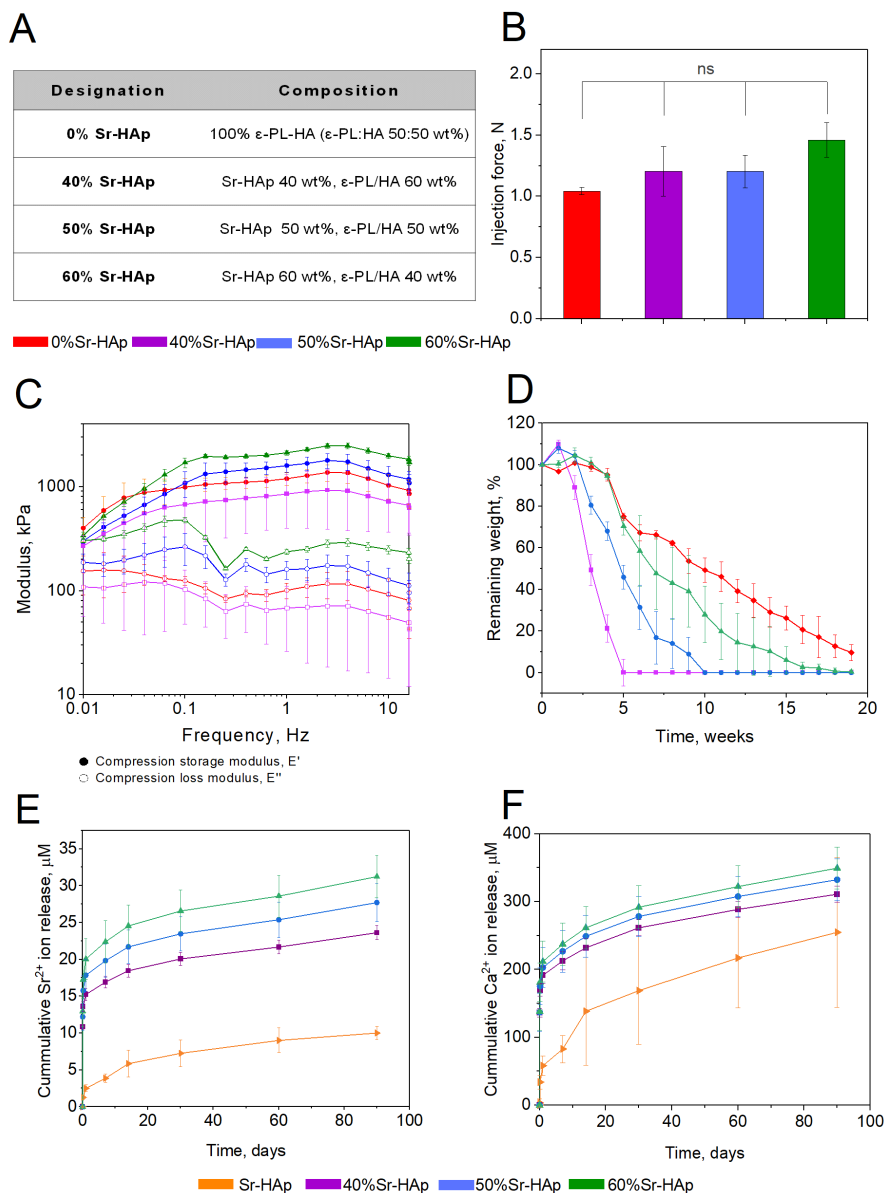


Figure 9. Physicochemical characterisation studies of the Sr-HAp/ $\epsilon$ -PL/HA hydrogels [72]. (A) Designation and composition of the Sr-HAp/ $\epsilon$ -PL/HA hydrogels used in subsequent experimental studies. (B) Injection force studies. No statistically significant differences (ns,  $p > 0.05$ ) in injection force values were found between the used compositions. (C) Compression studies within rheological investigation of the hydrogels. Compression tests were performed at 8 N axial force (axial force > dynamic force = 30 %), with 30  $\mu$ m axial displacement, over a frequency range from 0.01 to 16 Hz. Compression storage modulus ( $E'$ ) and compression loss modulus ( $E''$ ) were monitored. (D) Enzymatic degradation curves of the Sr-HAp/ $\epsilon$ -PL/HA hydrogels in hyaluronidase enzyme-containing PBS media over a 20-week period. (E)  $\text{Sr}^{2+}$  ion release studies. (F)  $\text{Ca}^{2+}$  ion release studies. (E–F) Ion release studies of Sr-HAp/ $\epsilon$ -PL/HA hydrogels performed over a 90-day period, with results presented in  $\mu\text{M}$  concentration. Three replicates were used in each experiment. Results are presented as mean  $\pm$  SD.

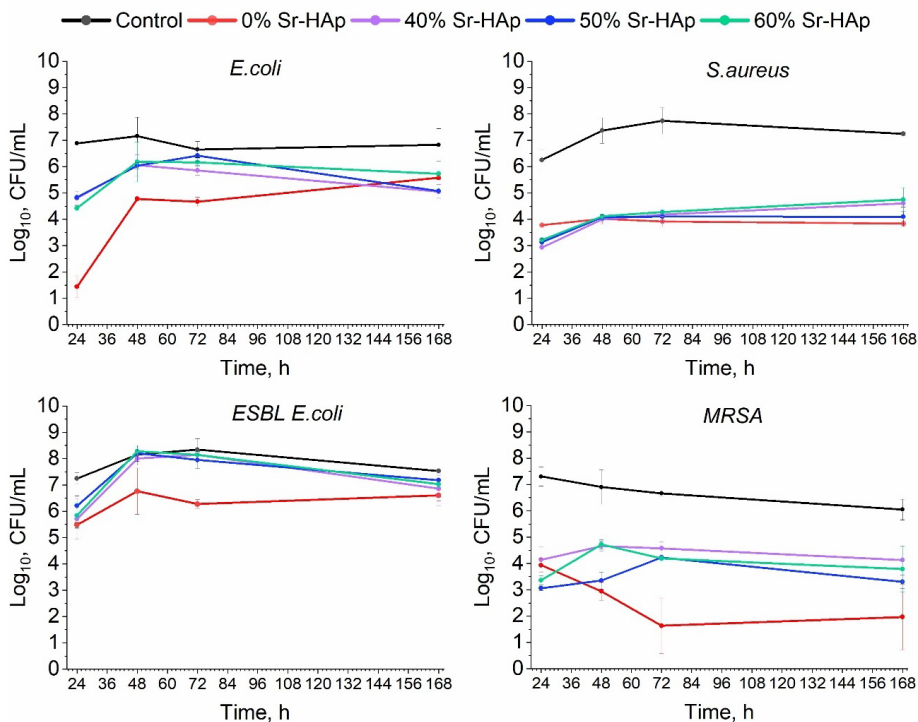


Figure 10. Antibacterial activity (24–168 h) of the as-prepared Sr-HAp/ε-PL/HA hydrogels against *E. coli*, *S. aureus*, ESBL *E. coli*, and MRSA ( $n = 3$ ) [72].

As previously hypothesised, a possible explanation could rely on the unique cell wall structure of Gram-negative bacteria and their more effective efflux systems. Thirdly, it was clearly observed that 0% Sr-HAp hydrogel composition at several time points (*E. coli*: 24 h; MRSA: 72 h), and in some cases, was the only composition showing statistically significant inhibition (*E. coli*: 24 h; MRSA: 72 h; (*E. coli*: 48 h and 72 h; ESBL *E. coli*: 48 h and 72 h). This may be explained by the presence of the Sr-HAp inorganic phase in the hydrogel matrix of the 40 %, 50 % and 60 % Sr-HAp hydrogel compositions. The functionalisation with Sr-HAp nanoparticles increases physical entanglements between the ε-PL/HA hydrogel matrix and positively charged  $\text{Ca}^{2+}/\text{Sr}^{2+}$  ions, forms a physical barrier and provokes network reorganisation into a more compact configuration. This negatively affects the release kinetics of antibacterial molecules of ε-PL and results in reduced antibacterial potential of hydrogels [74]. Finally, no statistically significant difference ( $p > 0.05$ ) was observed between the 40 %, 50 % and 60 % Sr-HAp hydrogels at any of the tested time points, suggesting that the presence of Sr-HAp did not significantly influence the antibacterial activity of the developed Sr-HAp/ε-PL/HA hydrogels.

## CONCLUSIONS

1. A reproducible synthesis methodology has been developed to fabricate chemically crosslinked, injectable  $\epsilon$ -PL/HA hydrogels using EDC/NHS (0.24:0.24 mol) chemistry, with  $\epsilon$ -PL to HA mass ratios of 40:60, 50:50, 60:40, 70:30, and 80:20 wt%.
2. The developed  $\epsilon$ -PL/HA hydrogels exhibit key properties relevant for antibacterial applications in tissue engineering, including tuneable free  $\epsilon$ -amino group content (via  $\epsilon$ -PL mass ratio), gel fraction stability (50–60 %), mechanical stiffness within the 5–15 kPa, smooth surface topology, injectability through a 19 G needle, high recovery after injection (85–95 %), and autoclavability at 121 °C for 20 min. These features contribute to dose-dependent antibacterial activity, achieving 2.3 Log<sub>10</sub> reduction in *E. coli* MSCL 332 after 1 h of contact.
3. Steam sterilisation at 121 °C for 20 min have not significantly affected gel fraction ( $p > 0.05$ ), pore size distribution (66–200  $\mu$ m), swelling (150–300 % within 2 h, swelling equilibrium after 4 h) and mechanical stiffness, while maintaining an antibacterial activity with 4–9 Log<sub>10</sub> bacterial reduction after sterilisation.
4.  $\epsilon$ -PL/HA hydrogels have demonstrated  $\epsilon$ -PL dose-dependent antibacterial activity in both fast (up to 24 h) and sustained (up to 168 h) timeframes, via direct and indirect contact, against *E. coli*, *S. aureus*, *P. aeruginosa*, as well as clinically relevant multidrug-resistant strains MRSA, and ESBL *E. coli*. No bacterial resistance has been observed against  $\epsilon$ -PL in reference or multidrug-resistant strains over 10 passages during a 1-month exposure period.
5. Cytotoxicity assays have demonstrated 70–90% cell viability for  $\epsilon$ -PL/HA hydrogels in Balb/c 3T3 mouse fibroblasts, with the IC<sub>50</sub> of pure  $\epsilon$ -PL determined as 4.21 mg/mL. Indirect extract-based cytotoxicity assays on human dermal fibroblasts (HDFs) have confirmed non-cytotoxicity at extract concentrations  $\leq 4.35$  mg/mL, supporting the  $\epsilon$ -PL dose-dependent biocompatibility of the developed hydrogel systems.
6. Sr-HAp/ $\epsilon$ -PL/HA hydrogels have been successfully developed and demonstrated a synergistic effect between  $\epsilon$ -PL/HA hydrogels and the Sr-HAp nanoparticles, resulting in sustained release of Sr<sup>2+</sup> ions (20–30  $\mu$ M) and Ca<sup>2+</sup> ions (200–350  $\mu$ M) over 90 days, retained injectability, tuneable enzymatic degradation depending on Sr-HAp content (complete degradation within 5–20 weeks). The composite hydrogels have exhibited fast-acting antibacterial activity (after 24 h) against both reference and multidrug-resistant bacteria strains, and prolonged efficacy (up to 168 h), particularly against *S. aureus* and clinically isolated multidrug-resistant MRSA.

## REFERENCES

- [1] 7.7 million people die from bacterial infections every year – 2022 – ReAct. <https://www.reactgroup.org/news-and-views/news-and-opinions/year-2022/7-7-million-people-die-from-bacterial-infections-every-year/> (accessed 2025-02-19).
- [2] Sceglovs, A.; Skadins, I.; Siverino, C.; Pirsko, V.; Sceglova, M.; Moriarty, F. T.; Kroica, J.; Salma-Ancane, K. Injectable  $\epsilon$ -Polylysine/Hyaluronic Acid Hydrogels with Resistance-Preventing Antibacterial Activity for Treating Wound Infections. *ACS Appl. Bio Mater.*, **2025**, *8* (11), 9916–9930. <https://doi.org/10.1021/acsabm.5c01252>.
- [3] Bilal, M.; Iqbal, H. M. N. Naturally-Derived Biopolymers: Potential Platforms for Enzyme Immobilization. *Int. J. Biol. Macromol.* **2019**, *130*, 462–482. <https://doi.org/10.1016/J.IJBIOMAC.2019.02.152>.
- [4] Sceglovs, A.; Skadins, I.; Chitto, M.; Kroica, J.; Salma-Ancane, K. Failure or Future? Exploring Alternative Antibacterials: A Comparative Analysis of Antibiotics and Naturally Derived Biopolymers. *Front. Microbiol.* **2025**, *16*, 1526250. <https://doi.org/10.3389/FMICB.2025.1526250>.
- [5] Sun, Y.; Bai, Y.; Yang, W.; Bu, K.; Tanveer, S. K.; Hai, J. Global Trends in Natural Biopolymers in the 21st Century: A Scientometric Review. *Front. Chem.* **2022**, *10*, 915648. <https://doi.org/10.3389/FCHEM.2022.915648>.
- [6] Pahlevanzadeh, F.; Setayeshmehr, M.; Bakhsheshi-Rad, H. R.; Emadi, R.; Kharaziha, M.; Poursamar, S. A.; Ismail, A. F.; Sharif, S.; Chen, X.; Berto, F. A Review on Antibacterial Biomaterials in Biomedical Applications: From Materials Perspective to Bioinks Design. *Polym. 2022, Vol. 14, Page 2238* **2022**, *14* (11), 2238. <https://doi.org/10.3390/POLYM14112238>.
- [7] Sam, S.; Joseph, B.; Thomas, S. Exploring the Antimicrobial Features of Biomaterials for Biomedical Applications. *Results Eng.* **2023**, *17*, 100979. <https://doi.org/10.1016/J.RINENG.2023.100979>.
- [8] Coma, V. Polysaccharide-Based Biomaterials with Antimicrobial and Antioxidant Properties. *Polimeros* **2013**, *23* (3), 287–297. <https://doi.org/10.4322/POLIMEROS020OV002>.
- [9] Khara, J. S.; Mojsoska, B.; Mukherjee, D.; Langford, P. R.; Robertson, B. D.; Jenssen, H.; Ee, P. L. R.; Newton, S. M. Ultra-Short Antimicrobial Peptoids Show Propensity for Membrane Activity Against Multi-Drug Resistant Mycobacterium Tuberculosis. *Front. Microbiol.* **2020**, *11*, 515317. <https://doi.org/10.3389/FMICB.2020.00417>.
- [10] Jacobo-Delgado, Y. M.; Rodríguez-Carlos, A.; Serrano, C. J.; Rivas-Santiago, B. Mycobacterium Tuberculosis Cell-Wall and Antimicrobial Peptides: A Mission Impossible? *Front. Immunol.* **2023**, *14*, 1194923.

- <https://doi.org/10.3389/FIMMU.2023.1194923>.
- [11] Intorasoot, S.; Intorasoot, A.; Tawteamwong, A.; Butr-Indr, B.; Phunpae, P.; Tharinjaroen, C. S.; Wattananandkul, U.; Sangboonruang, S.; Khantipongse, J. In Vitro Antimycobacterial Activity of Human Lactoferrin-Derived Peptide, D-HLF 1-11, against Susceptible and Drug-Resistant Mycobacterium Tuberculosis and Its Synergistic Effect with Rifampicin. *Antibiot.* 2022, Vol. 11, Page 1785 **2022**, 11 (12), 1785. <https://doi.org/10.3390/ANTIBIOTICS11121785>.
- [12] C Reygaert, W. An Overview of the Antimicrobial Resistance Mechanisms of Bacteria. *AIMS Microbiol.* **2018**, 4 (3), 482–501. <https://doi.org/10.3934/MICROBIOL.2018.3.482>.
- [13] Sceglavs, A.; Wychowaniec, J. K.; Skadins, I.; Reinis, A.; Edwards-Gayle, C. J. C.; D’Este, M.; Salma-Ancane, K. Effect of Steam Sterilisation on Physico-Chemical Properties of Antibacterial Covalently Cross-Linked  $\epsilon$ -Polylysine/Hyaluronic Acid Hydrogels. *Carbohydr. Polym. Technol. Appl.* **2023**, 6, 100363. <https://doi.org/10.1016/J.CARPTA.2023.100363>.
- [14] Harvey, N.; Dennison, E.; Cooper, C. Osteoporosis: Impact on Health and Economics. *Nat. Rev. Rheumatol.* 2010 62 **2010**, 6 (2), 99–105. <https://doi.org/10.1038/nrrheum.2009.260>.
- [15] Sozen, T.; Ozisik, L.; Calik Basaran, N. An Overview and Management of Osteoporosis. *Eur. J. Rheumatol.* **2017**, 4 (1), 46–56. <https://doi.org/10.5152/EURJRHEUM.2016.048>.
- [16] Hou, X.; Zhang, L.; Zhou, Z.; Luo, X.; Wang, T.; Zhao, X.; Lu, B.; Chen, F.; Zheng, L. Calcium Phosphate-Based Biomaterials for Bone Repair. *J. Funct. Biomater.* 2022, **2022**, 13 (4), 187. <https://doi.org/10.3390/JFB13040187>.
- [17] Tozzi, G.; De Mori, A.; Oliveira, A.; Roldo, M. Composite Hydrogels for Bone Regeneration. *Mater.* 2016, **2016**, 9 (4), 267. <https://doi.org/10.3390/MA9040267>.
- [18] Zhang, Y.; Shu, T.; Wang, S.; Liu, Z.; Cheng, Y.; Li, A.; Pei, D. The Osteoinductivity of Calcium Phosphate-Based Biomaterials: A Tight Interaction With Bone Healing. *Front. Bioeng. Biotechnol.* **2022**, 10, 911180. <https://doi.org/10.3389/FBIOE.2022.911180>.
- [19] Inzana, J. A.; Schwarz, E. M.; Kates, S. L.; Awad, H. A. Biomaterials Approaches to Treating Implant-Associated Osteomyelitis. *Biomaterials* **2016**, 81, 58–71. <https://doi.org/10.1016/J.BIOMATERIALS.2015.12.012>.
- [20] van Vugt, T. A. G.; Arts, J. J.; Geurts, J. A. P. Antibiotic-Loaded Polymethylmethacrylate Beads and Spacers in Treatment of Orthopedic Infections and the Role of Biofilm Formation. *Front. Microbiol.* **2019**, 10. <https://doi.org/10.3389/FMICB.2019.01626>.

- [21] Freischmidt, H.; Armbruster, J.; Reiter, G.; Grützner, P. A.; Helbig, L.; Guehring, T. Individualized Techniques of Implant Coating with an Antibiotic-Loaded, Hydroxyapatite/Calcium Sulphate Bone Graft Substitute. *Ther. Clin. Risk Manag.* **2020**, *16*, 689–694. <https://doi.org/10.2147/TCRM.S242088>.
- [22] Dovedytis, M.; Liu, Z. J.; Bartlett, S. Hyaluronic Acid and Its Biomedical Applications: A Review. *Eng. Regen.* **2020**, *1*, 102–113. <https://doi.org/10.1016/J.ENGREG.2020.10.001>.
- [23] Wang, M.; Deng, Z.; Guo, Y.; Xu, P. Designing Functional Hyaluronic Acid-Based Hydrogels for Cartilage Tissue Engineering. *Mater. Today Bio* **2022**, *17*, 100495. <https://doi.org/10.1016/J.MTBIO.2022.100495>.
- [24] Salma-Ancane, K.; Sceglavs, A.; Tracuma, E.; Wychowaniec, J. K.; Aunina, K.; Ramata-Stunda, A.; Nikolajeva, V.; Loca, D. Effect of Crosslinking Strategy on the Biological, Antibacterial and Physicochemical Performance of Hyaluronic Acid and  $\epsilon$ -Polylysine Based Hydrogels. *Int. J. Biol. Macromol.* **2022**, *208*, 995–1008. <https://doi.org/10.1016/J.IJBIOMAC.2022.03.207>.
- [25] Sionkowska, A.; Kulka-Kamińska, K.; Brudzyńska, P.; Lewandowska, K.; Piwowski, Ł. The Influence of Various Crosslinking Conditions of EDC/NHS on the Properties of Fish Collagen Film. *Mar. Drugs* **2024**, *22* (5), 194. <https://doi.org/10.3390/MD22050194>.
- [26] Munir, M. U.; Salman, S.; Javed, I.; Bukhari, S. N. A.; Ahmad, N.; Shad, N. A.; Aziz, F. Nano-Hydroxyapatite as a Delivery System: Overview and Advancements. *Artif. Cells, Nanomedicine, Biotechnol.* **2021**, *49* (1), 717–727. <https://doi.org/10.1080/21691401.2021.2016785>.
- [27] Lee, N. H.; Kang, M. S.; Kim, T. H.; Yoon, D. S.; Mandakhbayar, N.; Jo, S. Bin; Kim, H. S.; Knowles, J. C.; Lee, J. H.; Kim, H. W. Dual Actions of Osteoclastic-Inhibition and Osteogenic-Stimulation through Strontium-Releasing Bioactive Nanoscale Cement Imply Biomaterial-Enabled Osteoporosis Therapy. *Biomaterials* **2021**, *276*, 121025. <https://doi.org/10.1016/J.BIOMATERIALS.2021.121025>.
- [28] Pan, H. B.; Li, Z. Y.; Lam, W. M.; Wong, J. C.; Darvell, B. W.; Luk, K. D. K.; Lu, W. W. Solubility of Strontium-Substituted Apatite by Solid Titration. *Acta Biomater.* **2009**, *5* (5), 1678–1685. <https://doi.org/10.1016/J.ACTBIO.2008.11.032>.
- [29] Stipnice, L.; Wilson, S.; Curran, J. M.; Chen, R.; Salma-Ancane, K.; Sharma, P. K.; Meenan, B. J.; Boyd, A. R. Strontium Substituted Hydroxyapatite Promotes Direct Primary Human Osteoblast Maturation. *Ceram. Int.* **2021**, *47* (3), 3368–3379. <https://doi.org/10.1016/J.CERAMINT.2020.09.182>.
- [30] Stipnice, L.; Ramata-Stunda, A.; Vecstaudza, J.; Kreicberga, I.; Livkisa, D.; Rubina, A.;

- Sceglavs, A.; Salma-Ancane, K. A Comparative Study on Physicochemical Properties and In Vitro Biocompatibility of Sr-Substituted and Sr Ranelate-Loaded Hydroxyapatite Nanoparticles. *ACS Appl. Bio Mater.* **2023**, *6* (12), 5264–5281. <https://doi.org/10.1021/ACSABM.3C00539>.
- [31] Kołodziejaska, B.; Stępień, N.; Kolmas, J. The Influence of Strontium on Bone Tissue Metabolism and Its Application in Osteoporosis Treatment. *Int. J. Mol. Sci.* **2021**, *22* (12), 6564. <https://doi.org/10.3390/IJMS22126564>.
- [32] Rocha Scardueli, C.; Bizelli-Silveira, C.; Adriana Marcantonio, R. C.; Marcantonio Jr, E.; Stavropoulos, A.; Spin-Neto, R. Systemic Administration of Strontium Ranelate to Enhance the Osseointegration of Implants: Systematic Review of Animal Studies. *Int. J. Implant Dent.* **2018**, *4* (1), 1–9. <https://doi.org/10.1186/S40729-018-0132-8>.
- [33] Akram, F.; Imtiaz, M.; Haq, I. ul. Emergent Crisis of Antibiotic Resistance: A Silent Pandemic Threat to 21st Century. *Microb. Pathog.* **2023**, *174*, 105923. <https://doi.org/10.1016/J.MICPATH.2022.105923>.
- [34] *New report calls for urgent action to avert antimicrobial resistance crisis.* <https://www.who.int/news/item/29-04-2019-new-report-calls-for-urgent-action-to-avert-antimicrobial-resistance-crisis> (accessed 2024-04-02).
- [35] Muñoz-Bonilla, A.; Fernández-García, M. Polymeric Materials with Antimicrobial Activity. *Prog. Polym. Sci.* **2012**, *37* (2), 281–339. <https://doi.org/10.1016/J.PROGPOLYMSCI.2011.08.005>.
- [36] Santos, M. R. E.; Fonseca, A. C.; Mendonça, P. V.; Branco, R.; Serra, A. C.; Morais, P. V.; Coelho, J. F. J. Recent Developments in Antimicrobial Polymers: A Review. *Mater.* **2016**, *9* (7), 599. <https://doi.org/10.3390/MA9070599>.
- [37] Haktaniyan, M.; Bradley, M. Polymers Showing Intrinsic Antimicrobial Activity. *Chem. Soc. Rev.* **2022**, *51* (20), 8584–8611. <https://doi.org/10.1039/D2CS00558A>.
- [38] Smola-Dmochowska, A.; Lewicka, K.; Macyk, A.; Rychter, P.; Pamuła, E.; Dobrzyński, P. Biodegradable Polymers and Polymer Composites with Antibacterial Properties. *Int. J. Mol. Sci.* **2023**, *24* (8), 7473. <https://doi.org/10.3390/IJMS24087473>.
- [39] Mishra, R.; Panda, A. K.; De Mandal, S.; Shakeel, M.; Bisht, S. S.; Khan, J. Natural Anti-Biofilm Agents: Strategies to Control Biofilm-Forming Pathogens. *Front. Microbiol.* **2020**, *11*, 566325. <https://doi.org/10.3389/FMICB.2020.566325>.
- [40] Melander, R. J.; Basak, A. K.; Melander, C. Natural Products as Inspiration for the Development of Bacterial Antibiofilm Agents. *Nat. Prod. Rep.* **2020**, *37* (11), 1454–1477. <https://doi.org/10.1039/D0NP00022A>.
- [41] Munita, J. M.; Arias, C. A. Mechanisms of Antibiotic Resistance. *Microbiol. Spectr.* **2016**, *4* (2). <https://doi.org/10.1128/MICROBIOLSPEC.VMBF-0016-2015>.

- [42] Peterson, E.; Kaur, P. Antibiotic Resistance Mechanisms in Bacteria: Relationships between Resistance Determinants of Antibiotic Producers, Environmental Bacteria, and Clinical Pathogens. *Front. Microbiol.* **2018**, *9* (NOV), 426686. <https://doi.org/10.3389/FMICB.2018.02928>.
- [43] Abushaheen, M. A.; Muzaaheed; Fatani, A. J.; Alosaimi, M.; Mansy, W.; George, M.; Acharya, S.; Rathod, S.; Divakar, D. D.; Jhugroo, C.; Vellappally, S.; Khan, A. A.; Shaik, J.; Jhugroo, P. Antimicrobial Resistance, Mechanisms and Its Clinical Significance. *Dis. Mon.* **2020**, *66* (6). <https://doi.org/10.1016/J.DISAMONTH.2020.100971>.
- [44] Chamidah, A.; Hardoko; Prihanto, A. A. Antibacterial Activities of  $\beta$ -Glucan (Laminaran) against Gram-Negative and Gram-Positive Bacteria. *AIP Conf. Proc.* **2017**, *1844* (1), 20011. <https://doi.org/10.1063/1.4983422/748336>.
- [45] Hyldgaard, M.; Mygind, T.; Vad, B. S.; Stenvang, M.; Otzen, D. E.; Meyer, R. L. The Antimicrobial Mechanism of Action of Epsilon-Poly-L-Lysine. *Appl. Environ. Microbiol.* **2014**, *80* (24), 7758–7770. <https://doi.org/10.1128/AEM.02204-14>.
- [46] Janssen, H.; Hancock, R. E. W. Antimicrobial Properties of Lactoferrin. *Biochimie* **2009**, *91* (1), 19–29. <https://doi.org/10.1016/J.BIOCHI.2008.05.015>.
- [47] Vedadghavami, A.; Minoee, F.; Mohammadi, M. H.; Khetani, S.; Rezaei Kolahchi, A.; Mashayekhan, S.; Sanati-Nezhad, A. Manufacturing of Hydrogel Biomaterials with Controlled Mechanical Properties for Tissue Engineering Applications. *Acta Biomater.* **2017**, *62*, 42–63. <https://doi.org/10.1016/J.ACTBIO.2017.07.028>.
- [48] Bai, X.; Gao, M.; Syed, S.; Zhuang, J.; Xu, X.; Zhang, X. Q. Bioactive Hydrogels for Bone Regeneration. *Bioact. Mater.* **2018**, *3* (4), 401–417. <https://doi.org/10.1016/J.BIOACTMAT.2018.05.006>.
- [49] Moreira, C. D. F.; Carvalho, S. M.; Florentino, R. M.; França, A.; Okano, B. S.; Rezende, C. M. F.; Mansur, H. S.; Pereira, M. M. Injectable Chitosan/Gelatin/Bioactive Glass Nanocomposite Hydrogels for Potential Bone Regeneration: In Vitro and in Vivo Analyses. *Int. J. Biol. Macromol.* **2019**, *132*, 811–821. <https://doi.org/10.1016/J.IJBIOMAC.2019.03.237>.
- [50] Cross, E. R.; Coulter, S. M.; Pentlavalli, S.; Laverty, G. Unravelling the Antimicrobial Activity of Peptide Hydrogel Systems: Current and Future Perspectives. *Soft Matter* **2021**, *17* (35), 8001–8021. <https://doi.org/10.1039/D1SM00839K>.
- [51] Qu, H.; Yao, Q.; Chen, T.; Wu, H.; Liu, Y.; Wang, C.; Dong, A. Current Status of Development and Biomedical Applications of Peptide-Based Antimicrobial Hydrogels. *Adv. Colloid Interface Sci.* **2024**, *325*, 103099. <https://doi.org/10.1016/J.CIS.2024.103099>.
- [52] Wang, R.; Xu, D.; Liang, L.; Xu, T.; Liu, W.; Ouyang, P.; Chi, B.; Xu, H. Enzymatically

- Crosslinked Epsilon-Poly-L-Lysine Hydrogels with Inherent Antibacterial Properties for Wound Infection Prevention. *RSC Adv.* **2016**, *6* (11), 8620–8627. <https://doi.org/10.1039/C5RA15616E>.
- [53] Zou, Y. J.; He, S. S.; Du, J. Z.  $\epsilon$ -Poly(L-Lysine)-Based Hydrogels with Fast-Acting and Prolonged Antibacterial Activities. *Chinese J. Polym. Sci. (English Ed.)* **2018**, *36* (11), 1239–1250. <https://doi.org/10.1007/S10118-018-2156-1>.
- [54] Kennedy, S. M.; Deshpande, P.; Gallagher, A. G.; Horsburgh, M. J.; Allison, H. E.; Kaye, S. B.; Wellings, D. A.; Williams, R. L. Antimicrobial Activity of Poly-Epsilon-Lysine Peptide Hydrogels Against *Pseudomonas Aeruginosa*. *Invest. Ophthalmol. Vis. Sci.* **2020**, *61* (10), 18–18. <https://doi.org/10.1167/IOVS.61.10.18>.
- [55] Wang, L.; Zhang, C.; Zhang, J.; Rao, Z.; Xu, X.; Mao, Z.; Chen, X. Epsilon-Poly-L-Lysine: Recent Advances in Biomanufacturing and Applications. *Front. Bioeng. Biotechnol.* **2021**, *9*, 895. <https://doi.org/10.3389/FBIOE.2021.748976>.
- [56] Tan, Z.; Shi, Y.; Xing, B.; Hou, Y.; Cui, J.; Jia, S. The Antimicrobial Effects and Mechanism of  $\epsilon$ -Poly-Lysine against *Staphylococcus Aureus*. *Bioresour. Bioprocess.* **2019**, *6* (1). <https://doi.org/10.1186/s40643-019-0246-8>.
- [57] Li, Y.; Wang, Y.; Li, J. Antibacterial Activity of Polyvinyl Alcohol (PVA)/ $\epsilon$ -Polylysine Packaging Films and the Effect on Longan Fruit. *Food Sci. Technol.* **2020**, *40* (4), 838–843. <https://doi.org/10.1590/FST.19919>.
- [58] Amorim, S.; Reis, C. A.; Reis, R. L.; Pires, R. A. Extracellular Matrix Mimics Using Hyaluronan-Based Biomaterials. *Trends Biotechnol.* **2021**, *39* (1), 90–104. <https://doi.org/10.1016/J.TIBTECH.2020.06.003>.
- [59] Harrer, D.; Sanchez Armengol, E.; Friedl, J. D.; Jalil, A.; Jelkmann, M.; Leichner, C.; Laffleur, F. Is Hyaluronic Acid the Perfect Excipient for the Pharmaceutical Need? *Int. J. Pharm.* **2021**, *601*, 120589. <https://doi.org/10.1016/J.IJPHARM.2021.120589>.
- [60] Guo, W.; Douma, L.; Hu, M. H.; Eglin, D.; Alini, M.; Šćecerović, A.; Grad, S.; Peng, X.; Zou, X.; D'Este, M.; Peroglio, M. Hyaluronic Acid-Based Interpenetrating Network Hydrogel as a Cell Carrier for Nucleus Pulposus Repair. *Carbohydr. Polym.* **2022**, *277*, 118828. <https://doi.org/10.1016/J.CARBPOL.2021.118828>.
- [61] Hu, W.; Wang, Z.; Xiao, Y.; Zhang, S.; Wang, J. Advances in Crosslinking Strategies of Biomedical Hydrogels. *Biomater. Sci.* **2019**, *7* (3), 843–855. <https://doi.org/10.1039/c8bm01246f>.
- [62] Cui, H.; Zhuang, X.; He, C.; Wei, Y.; Chen, X. High Performance and Reversible Ionic Polypeptide Hydrogel Based on Charge-Driven Assembly for Biomedical Applications. *Acta Biomater.* **2015**, *11* (1), 183–190. <https://doi.org/10.1016/J.ACTBIO.2014.09.017>.
- [63] Xue, X.; Hu, Y.; Wang, S.; Chen, X.; Jiang, Y.; Su, J. Fabrication of Physical and

- Chemical Crosslinked Hydrogels for Bone Tissue Engineering. *Bioact. Mater.* **2022**, *12*, 327–339. <https://doi.org/10.1016/J.BIOACTMAT.2021.10.029>.
- [64] Hua, J.; Li, Z.; Xia, W.; Yang, N.; Gong, J.; Zhang, J.; Qiao, C. *Preparation and Properties of EDC/NHS Mediated Crosslinking Poly (Gamma-Glutamic Acid)/Epsilon-Polylysine Hydrogels*; Elsevier B.V., 2016; Vol. 61. <https://doi.org/10.1016/j.msec.2016.01.001>.
- [65] Porod, G. *General Theory - Small Angle X-Ray Scattering*; Glatter, O. . K. O., Ed.; Academic Press: London, 1982.
- [66] *M07 Ed12 | Methods for Dilution Antimicrobial Susceptibility Tests for Bacteria That Grow Aerobically, 12<sup>th</sup> Edition*. <https://clsi.org/standards/products/microbiology/documents/m07/> (accessed 2025-02-19).
- [67] *ISO 10993-5:2009 - Biological evaluation of medical devices — Part 5: Tests for in vitro cytotoxicity*. <https://www.iso.org/standard/36406.html> (accessed 2025-02-27).
- [68] Burguera, E. F.; Xu, H. H. K.; Sun, L. Injectable Calcium Phosphate Cement: Effects of Powder-to-Liquid Ratio and Needle Size. *J. Biomed. Mater. Res. Part B Appl. Biomater.* **2008**, *84B* (2), 493–502. <https://doi.org/10.1002/JBM.B.30896>.
- [69] Jacquart, S.; Girod-Fullana, S.; Brouillet, F.; Pigasse, C.; Siadous, R.; Fatnassi, M.; Grimoud, J.; Rey, C.; Roques, C.; Combes, C. Injectable Bone Cement Containing Carboxymethyl Cellulose Microparticles as a Silver Delivery System Able to Reduce Implant-Associated Infection Risk. *Acta Biomater.* **2022**, *145*, 342–357. <https://doi.org/10.1016/J.ACTBIO.2022.04.015>.
- [70] Baniasadi, M.; Minary-Jolandan, M.; Editor, A.; Zadpoor, A. A. Alginate-Collagen Fibril Composite Hydrogel. *Mater.* *2015*, **2015**, *8* (2), 799–814. <https://doi.org/10.3390/MA8020799>.
- [71] Liu, L.; Cooke, P. H.; Coffin, D. R.; Fishman, M. L.; Hicks, K. B. Pectin and Polyacrylamide Composite Hydrogels: Effect of Pectin on Structural and Dynamic Mechanical Properties. *J. Appl. Polym. Sci.* **2004**, *92* (3), 1893–1901. <https://doi.org/10.1002/APP.20174>.
- [72] Rubina, A.; Sceglavs, A.; Ramata-Stunda, A.; Pugajeva, I.; Skadins, I.; Boyd, A. R.; Tumilovica, A.; Stipniece, L.; Salma-Ancane, K. Injectable Mineralized Sr-Hydroxyapatite Nanoparticles-Loaded  $\epsilon$ -Polylysine-Hyaluronic Acid Composite Hydrogels for Bone Regeneration. *Int. J. Biol. Macromol.* **2024**, *280*, 135703. <https://doi.org/10.1016/J.IJBIOMAC.2024.135703>.
- [73] Karvinen, J.; Kellomäki, M. Characterization of Self-Healing Hydrogels for Biomedical Applications. *Eur. Polym. J.* **2022**, *181*, 111641.

<https://doi.org/10.1016/J.EURPOLYMJ.2022.111641>.

- [74] Murugesan, V.; Vaiyapuri, M.; Murugesan, A. Fabrication and Characterization of Strontium Substituted Chitosan Modify Hydroxyapatite for Biomedical Applications. *Inorg. Chem. Commun.* **2022**, *142*, 109653. <https://doi.org/10.1016/J.INOCHE.2022.109653>.



**Artemijs Ščeglovs** was born in 1996 in Riga, Latvia. In 2019, he obtained a Bachelor's degree in Chemistry from Riga Technical University (RTU), and a Master's degree in Biomedicine – from Riga Stradiņš University in 2021. At present, Artemijs is as a Researcher at RTU. He is involved in the implementation of national and international projects, participating in international conferences across Europe and enhancing his professional experience through training and mobility visits. Research interests are related to the development of biomaterials with a focus on antibacterial activity against various disease-causing, including antibiotic-resistant, bacteria.